CR-184171

EASTERN KENTUCKY UNIVERSITY

Department of Physics and Astronomy

Study of Activation of Metal Samples from LDEF-1 and Spacelab-2

July, 1991

Final Technical Report

Contract # NAS8-36649

(Principal Investigator: C. E. Laird)

Prepared for

George C. Marshall Space Flight Center

Marshall Space Flight Center, Alabama 35812

EASTERN KENTUCKY UNIVERSITY

Richmond, Kentucky 40475

STUDY OF ACTIVATION OF METAL SAMPLES FROM LDEF-1 AND SPACELAB-2.

NASA CONTRACT NAS8-36647

BY

C. E. Laird, Ph.D.
Professor of Physics
Eastern Kentucky University

ABSTRACT

The activation of metal samples and other material orbited onboard LDEF-1 and Spacelab-2 have been studied. Measurements of the radioactivities of spacecraft material have been made and corrections for self-absorption and efficiency have been calculated. Activation cross sections for specific metal samples have been updated while cross sections for other materials have been tabulated from the scientific literature. Activation cross sections for 200 MeV neutrons have been experimentally determined. Linear absorption coefficients, half lives, branching ratios and other pertinent technical data needed for LDEF-sample analyses have been tabulated. The current status of the sample counting at low background facilities at national laboratories has been reported. The Appendix contains detailed calculations of the activation of the LDEF materials.

CONTENTS

List of Tables

List of Figures

Final Technical Report

Contract NAS8-36647

INTRODUCTION

The long Duration Exposure Facility (LDEF) was placed in orbit in April 1984 for an expected one-year mission. Because of the Challenger accident and subsequent delays, the recovery of LDEF was not achieved until February 1990--almost six years from insertion into orbit. Aboard the facility were approximately twenty specifically chosen "intentional" metal samples made from five elements--vandium, nickel, cobalt, indium and tantalum. These samples originally were 2" x 2" x 1/8" in dimension but some were cut in half to accommodate placement among the various experimental trays. The intent of this experiment was to obtain bulk-activation measurements from the samples activated by protons trapped in the magnetic field of the Earth, by neutrons and by other activating particles such as cosmic rays. After retrieval, gamma-ray counting was done on these and other samples at several low-background counting facilities. At this time this counting continues.

The contract NAS8-36647 was initiated to provide scientific support to the interpretation of the data from these samples and was later modified to include analysis for other metallic samples such as stainless steel, aluminum and titanium removed from the spacecraft. These "unintentional" samples are also being counted at low-background gamma-ray counting facilities. Supplemental information on this work can be found in the Final Technical Report of Contract #NAS8-35180, July, 1985.

The original statement of work for this contract is as follows:

The contractor shall perform the following studies and provide calculations related to the induced radioactivity of metal samples returned from the LDEF-1 and Spacelab 2 missions.

1. Using gamma-ray spectra obtained post-flight from the samples at EKU and/or MSFC, derive the net activities due to radioisotopes detected in the samples. Corrections for geometry, self-absorption, detector efficiency and background shall be made. Uncertainties of the net rate due to counting statistics and experimental errors shall be estimated.

2. The saturation activity, averaged over the mission, shall be determined for each radioisotope, measured in disintegrations per second per kilogram of material.

3. Activation cross-sections shall be determined for 200 MeV neutrons incident on various metal samples from data collected at the Indiana University Cyclotron Facility.

4. Using the above cross sections and those obtained from the scientific literature, estimates shall be made of the fluxes of activating protons and neutrons, averaged over the mission lifetime, at various locations within the LDEF and Spacelab 2 spacecrafts.

The Statement of Work was modified in 1990 to read as follows:

Paragraph 1 of the Statement of Work (p.J-1-1), Attachment J-1 shall be deleted and the following paragraph shall be substituted in its place:

1. Obtain an updated compilation of nuclear reaction cross-sections relevant to the LDEF studies. Using gamma-ray spectra obtained in the Space Science Laboratory, Marshall Space Flight Center and other government laboratories, perform analysis to determine the incident fluxes required to produce the observed activation. Corrections for geometry, self-absorption, detector efficiency and background shall be made. Uncertainties due to counting statistics and experimental errors shall be estimated. The results shall be documented in a final report.

In fulfillment of the statement of work this report includes the following:

1. Final results of the activation of five metal samples of vanadium, cobalt, nickel, indium and tantalum performed at the Indiana university Cyclotron Facility.

2. Additional cross sections found in the literature both for the "intentional" and "unintentional" samples.

3. Calculations of expected activation of parallelopiped samples using the incident fluxes reported for NAS8-35780, and a comparison with "completed" measurements of the samples including a brief analysis of the fluxes of incident particles activating the spacecraft material.

4. An analysis of the geometry, self-absorption, efficiency and background corrections for the low background counting facility at the Space Science Laboratory and a summary of the status of these corrections at other counting facilities. Included with this will be an analysis of the statistical and systematic errors of the data from the various counting sites.

5. A summary of the present status of the counting of the samples and of the data analysis as well as recommendations for additional analysis.

The results presented in this report are limited by the incomplete nature of the counting of the samples done at the many counting facilities. All of the counting and the reporting of the results by the facilities had not been completed by December 31, 1990. This limits the conclusions presented in this report.

A peripheral contribution from this and the previously funded study involving the LDEF1 Mission has been the involvement of students in the research project and the knowledge transferred and impression made on them and their contemporaries about the space

program. Over the past seven years at least seven graduate and three undergraduate students have participated in the research. At least one is currently employed in a space-related field of research and development. Furthermore, much of this same information has been disseminated by the Principal Investigator to his students in undergraduate as well as undergraduate classes. In one instance, the PI gave an hour presentation about LDEF1 and other NASA projects(HST, GRO, etc.) to a group of sixty French high school students visiting Eastern Kentucky University as a English language training program. Many other unknown benefits cannot be enumerated.

SECTION I

Activation of Thick Metal Samples with 200 MeV Neutrons

INTRODUCTION

The determination of the fluxes of activating particles and of the activation caused by these particles is extremely important in many physical experiments or observational facilities. These situations include not only fusion and fission reactors, but also orbiting space craft such as the Gamma Ray Observatory and the Space Station. The planning for the effective facility lifetime in such situations and the determination of the optimum amount of shielding and of the effects of radiation requires accurate estimation of the expected activation as well as for the flux of activating particles. In making determinations of the expected activation the prevailing mechanical stress, as in a satellite, precludes the use of thin foils. Furthermore, the physical effects in a thin foil does not effectively mirror the actual effects in the material. Therefore, thick samples of material are required to obtain meaningful data.

Making accurate measurements of weakly-activated thick samples has many technical problems that must be overcome. Since the samples are weakly activated, a low-background counting facility and a large solid angle are needed. However, a large solid angle for an non-point source produces problems with inverse-square effects on the detector efficiency and of self-absorption of the gamma rays within the sample. Also, in order to convert the activation into particle fluxes the cross sections for the reactions must be known. To effectively study the first problem and to obtain experimental data for the second we have activated several thick metallic samples to develop a model of the inverse-square and self-absorption effects and to determine the cross section for the interaction of high energy neutrons on these samples. This activation was done with the active support of Dr. Tom Ward(currently at the Radiation Effects Facility, Brookhaven National Laboratory) and the staff of the Indiana University Cyclotron Facility.

EXPERIMENTAL PROCEDURE

Metallic samples of Vanadium, Nickel, Cobalt, Indium, and Tantalum were activated with 200 MeV neutrons at the Indiana University Cyclotron Facility. The samples were elementally pure

with dimensions 5.08 x 5.08 x .3175 cm and were activated for a time of 988 minutes. The neutrons were produced by 200 MeV protons incident on a ^{7}Li target.[1] The samples were placed in the forward neutron direction with the proton beam being diverted by a clearing magnet. The neutron flux is expected to be quasimonoenergetic with a dominant peak and a flat low-energy tail.[2] The high-energy neutron flux was determined from the activation of 1/16 inch aluminum foils placed on either side of the samples. Neutron activation of Al by 200 MeV neutrons has a known cross section of 30 mb[3] for the production of ^{24}Mg. The yield of the 1368 keV gamma ray was used in determining the fast-neutron flux. The flux incident on each sample is given in Col. 2 of Table I-1.

The samples were counted with a gamma-ray spectrometer consisting of a Ge(Li) detector with appropriate electronics and multichannel analyzer. The detector efficiency was measured at 10 cm, at the center-face of the detector housing, and along the face at 2.54 cm from the cylindrical axis of the detector with a National Bureau of Standard calibrated gamma-ray source. This mixed gamma-ray source consisted of ^{125}Sb, ^{155}Eu, and ^{154}Eu allowing for an efficiency measurement for seventeen energies from 86.6 keV to 1596.5 keV. Except for the initial counting of the indium sample which was placed at 10 cm, samples were placed at the detector face and counted for varying time periods over three days. Each sample except tantalum was counted twice. The gamma spectra were analyzed with the computer code SAMPO.[4] The parent nuclei and the observed gamma rays are listed in Cols. 1 and 2 in Table I-2, respectively. Also listed in this table are the appropriate halflives and gamma branching ratios.[5]

Point Source Efficiency

For the point source at 10 cm the efficiency of the Ge(Li) was determined to an accuracy of better than 3% depending on the statistical uncertainty of the peak areas. Over the range from 86.6 to 1597 keV the efficiency data was fit to the function:

$$\ln(\varepsilon) = a/E_\gamma + b + c\ln(E_\gamma) + d(\ln(E_\gamma)^2 + e(\ln(E_\gamma))^3 \qquad (1)$$

where ε is the efficiency and E_γ is the energy of the gamma ray. The values of the chi-square minimization fit are

a = -564.919 +/- 16.98
b = 55.165807 +/- 2.42
c = -21.1216 +/- .984
d = 2.47916 +/- .1382
e = -.10143 +/- .0067

with a chi square per degree of freedom of 2.3. A better statement of the quality of fit is that the average deviation of the difference of the fit from the actual efficiency is 1.9% and is1.4% if the very weak 381 and 1597 keV peaks are eliminated. No other peak differs from the fit by more than 2.6%. Therefore, we take the accuracy of the efficiencies determined with this function to be 3%. Figure (I-1) shows the efficiency as a function of gamma-ray energy at 10 cm and the fit to Eq.(1).

The determination of the efficiency at the center of the detector face and at the corner suffers from cascade summing for the ^{154}Eu source. Cascade summing occurs when two or more gamma rays in a nuclear cascade are emitted in a correlated fashion within the resolving time of the detector system. The other two sources, ^{155}Eu and ^{125}Sb, do not significantly suffer from this problem because the gamma rays originate in different nuclear levels and proceed to the ground state. Therefore, the efficiency at the closer points were measured with these gamma rays. Excluding the ^{154}Eu source and the 87 keV gamma which is inconsistent with the other seven gamma ray, the ratios of the efficiencies to that at 10 cm is 14.5 +/- .3 for the center and 9.63 +/- .60 for 2.54 cm off axis. This corresponds to an effective source distance of 3.5 cm from the center position of this detector which has a surface area of 16.4 cm^2.

Extended Source Effects

The absolute determination of neutron fluxes and of reaction cross sections for extended sources requires correcting for the effects of self-absorption within the sample and for the reduction in detector efficiency caused by the distance from source to detector for various points within the sample. The calculation of such a correction is a straightforward process. The basic assumptions are that:

1. The sample is activated uniformly throughout its volume.

2. The efficiency of the detector falls off as the inverse square of the effective distance from the detector to the source.

Simple activation calculations show that the first assumption will be correct for reactions with cross sections of a few barns or less. The validity of the second condition is implied by the efficiency measurements in the previous section. Further validation of these assumption will be shown to be given by the internal consistancy found in the analysis of the activated samples.

The inverse-square and self-attenuation corrections are calculated by considering the sample as being made up of a large number of solid cells having the same dimensions. The activity of each cell is considered to be located at the center. The distance of the cell from the effective location of the detector is calculated to determine the inverse-square reduction in the efficiency. The perpendicular distance D from the point to the surface and the angle Θ between the line to the detector and a normal to the surface are calculated for each cell to determine the absorption distance through the sample. The absorption distance, through which photons must travel, is given by $D/(\cos \Theta)$. The attenuation is calculated using this distance and the linear absorption coefficient. The correction is calculated as a ratio to the efficiency of the detector for a source of a particular shape placed at a specific position. For this experiment the correction ratio was related to a point source on the detector axis at the surface of the detector housing. Figure I-2 gives a log-log plot of the inverse-square and absorption correction relative to the efficiency at the center of the detector surface. The estimated uncertainty in these corrections is 5% and is discussed in detail below.

RESULTS

Accuracy of Efficiency and Attenuation Corrections

Table I-3 contains the corrected gamma-ray yields for ^{182}Ta, ^{55}Co, ^{176}Ta, and ^{116m}In using gamma rays with branching ratios greater than 1%. Figure I-3 shows these realtive yields as a function of gamma-ray energy with Fig. (I-3e) giving a composite of all four for relative comparison. Tantalum-182 and ^{116m}In are produced by (n,γ) reactions while ^{55}Co is produced by the (n,pxn) reactions on nickel. The thick sample intensities for ^{182}Ta agree to better than 5% over the energy range from 100 keV to 1300 keV. The ^{55}Co intensities indicate an agreement to better than 10% and is consistent with the ^{182}Ta intensities. Except for the 138 keV gamma ray the corrected relative yields from ^{116m}In agree to about 8%. Because of the

greater gamma-ray yield from the Ta sample relative to the spectra from the other two samples and to the short mean free path for neutrons in indium, the uncertainty of the inverse-square and self-absorption correction is taken to be 5%. In fact, the scattered of data points in these figures implies a greater random error in the yields than in the correction.

Neutron radiative-capture, (n,γ), on tantalum, cobalt and indium indicates the presence of a significant low-energy(possibly thermal) neutron flux. The magnitude of that flux can be estimated from the gamma-ray yields from ^{182}Ta, ^{60}Co, and ^{116m}In. Table I-4 gives the average neutron fluxes assuming that the appropriate reaction cross sections are those for thermal neutrons. The fluxes calculated from the Ta and Co samples agree within a factor of 2.5 while the one for In differs by an order of magnitude. At least two factors contribute to this disagreement. First, the actual neutron flux is a continuum from 200 MeV to the thermal region(thermal neutrons are produced by the shielding material around the target cell) peaked near 200 MeV in the forward direction. Second, indium has a mean free path of .165 cm for thermal neutrons. The activation of the indium sample will therefore not be uniform throughout and the efficiency and attenuation corrections will not be valid.

Spectral Analyses

As with the efficiency data the gamma-ray spectra from the activated samples were analyzed using the computer code SAMPO. The resultant peak areas were reduced to cross sections using:

$$\sigma = Y_\gamma A/[N_A \phi t C \varepsilon f_\gamma \lambda^{-2}(1- e^{-\lambda T})(e^{-\lambda T_1} - e^{-\lambda T_2})] \qquad (2)$$

where Y_γ is the gamma-ray yield, ε is the detector efficiency at the center of the detector housing, C is the inverse-square and self-absorption correction, f_γ is the gamma-ray branching ration, λ is the decay constant for the decaying radioisotope, T is the bombardment time, T_1 is the time counting started and T_2 is the time counting ended, φ is the neutron flux, A is the atomic weight of the target, N_A is Avogadro's number, and t is the target area density. Except for the statistical uncertainty in the photopeak area the absolute total uncertainty is 12% and includes the uncertainties in the efficiency (3%), the inverse- square and self-absorption correction(5%), the neutron flux (10%), the target thickness (1%), branching ratios(as given in Table I-2), and the half-life (<1%).

Tables I- 5 give the results of these calculations. Listed with the cross sections are the photopeak uncertainties including those resulting from separating photopeak areas into those from competing decays (i.e. 984 from ^{48}V and ^{48}Sc decays). When two or more photopeaks are used in determining a cross section, the result given is a weighted average calculated inversely with respect to the square of the photopeak uncertainty. Except for tantalum, two spectra were taken from each sample and are reported in the tables as well as a weighted average of the two sets of results. The estimated total error is the error stated in the tables folded in quadrature with the 12% error previously stated.

Vanadium

Both ^{48}V and ^{48}Sc decay to ^{48}Ti emitting gamma rays of 984 and 1312 keV. Fortunately, ^{48}Sc also emits a 1037 keV gamma ray. The 1037 keV gamma-ray yield has been used to subtract out the ^{48}Sc contamination to the ^{48}V yields. The resulting cross sections are very consistent despite relatively large propagated statistical errors. With the possible exception of ^{46}Sc the other cross sections are consistent.

Cobalt

In addition to the possibility that ^{48}Sc would produce a 1037 keV gamma ray ^{56}Co also produces one. Therefore, the absence of a 1037 keV gamma ray in the spectrum could be interpreted as indicating the absence of both nuclei. However, a gamma ray may be present but below a practical "threshold" for detection. Furthermore, the presence of 846 and 1238 keV gamma rays shows that ^{56}Co is present. The absence of ^{48}Sc is both a "threshold" effect as well as the strong likelihood that it is much more probable for 4 protons and 12 neutrons will be emitted rather than 6 protons and 10 neutrons. This trend is indicated by the 4/1 ($^{48}V/^{48}Sc$) cross-sectional ratio for the vanadium target.

Nickel

Table I-7 gives the experimental neutron activation cross sections for nickel. The nuclides produced in these reactions are essentially the same as produced in cobalt. However, unlike cobalt the 1037 keV line from ^{48}Sc, or ^{56}Co, is present in one of the

countings. The production cross section is only 4% of the ^{48}V cross section. This confirms the assumption that ^{48}Sc cross section will be negligible for this target.

Indium

Table I-8 gives the experimental cross sections for the indium target. Unfortunately, most of the gamma ray yields produced in these reactions are not strong enough to give a large number of measurements. This can be due to half-lives being either so short that the nuclide has mostly decayed before measurements were made or so long that the activity is too low to provide sufficient yield for detection and measurement, or the production cross section is quite small. One interesting nuclide produced was ^{114m}In, but there is a question concerning whether this comes from (n,2n) on ^{115}In or (n,γ) on ^{113}In. The (n,γ) identification would correspond to a thermal neutron flux of 5.2×10^6 n/s/cm^2 which is higher than in the cases of tantalum and cobalt and thus may have a large non-thermal component, but is not sufficiently different to warrant acceptance as such.

Tantalum

Table I-9 gives the cross sections for the tantalum target obtained in this study. Unfortunately, the spectrum from the nuclides produced in this target contains a large number of ^{182}Ta peaks and several decays produce the same gamma rays, or gamma rays of almost the same energy. Furthermore, the presence of X rays as high as 67 keV in the spectrum complicates the analysis because of the significant possibility of summing. One particular set of decays stands out as a problem. The decays of ^{177}Lu and ^{177}Ta produce 112.9 and 208.4 keV gamma rays while ^{182}Ta produces a 113.7 keV gamma ray and ^{167}Ta produces a 207.8 keV gamma ray. Although the contribution from ^{182}Ta to the 113 keV peak can be subtracted from the photopeak area, separating the contributions from the other two decays(three including ^{167}Ta) can not be done because there are no other significant peaks onto which to normalize. Therefore, no cross-sectional entry has been made although the two mass 177 nuclei are definitely present.

Because of the interference of many different decays in the gamma spectrum, great care had to be made in selecting those to be included in cross-sectional calculations. Therefore, in Table I-9 the gamma rays used in this analysis have been listed. Whenever an

inconsistency was observed in the analysis, those having clear interference were excluded in the final results.

References for Section I

1. J. D'Auria, M. Dombsky, L. Moritz, T. Ruth, G. Sheffer, T. E. Ward, C. C. Foster, J. W. Watson, B. D. Anderson, and J. Rapaport, Phys. Rev. **30**, 1999(1984).

2. C. M. Castaneda, J. L. Ullman, F. P. Brady, J. L. Romero, N. S. P. King, M. Blann, Phys. Rev. C**28**, 1493(1983).

3. T. E. Ward, Radiation Effects Facility, Brookhaven National Laboratory, private communication.

4. J. T. Routti and S. G. Prussin, Nucl. Inst. and Methods **72**, 125(1969).

5. Edgardo Browne, Richard B. Firestone, and Virginia Shirley, Table of Radioactive Isotopes, John Wiley & Sons, 1986

Table I-1
Fast Neutron Flux

Sample	Flux(+/- 10%) (10^5 neutrons/sec/cm^2)
Cobalt	1.63
Indium	1.63
Nickel	1.46
Tantalum	1.55
Vanadium	1.23

Table I-2(a)

Nuclear Data used in the Evaluation of Cross Sections for Vanadium, Cobalt and Nickel.

Nuclide	Half-life (days)	E_γ (keV)	I_γ (%)	Target
^{42}K	.515	1524.9	.179	V
^{43}Sc				
^{43}K	.925	617.5	.80	V
		372.8	.702	
^{44}Sc	.16363	1157.	.9988	V,Co,Ni
^{44m}Sc	2.44	271.2	.866	V,Co,Ni
^{46}Sc	83.8	889.3	1.00	V,Co,Ni
		1120.5	1.00	
^{47}Sc	3.42	159.4	.685	V
^{48}Sc	1.82	1037.4	1.00	V
^{48}Cr	.898	112.5	.98	V,Ni
		308.3	.99	
^{48}V	15.98	984.	1.00	V,Co,Ni
		1312.	.99	
^{51}Cr	27.7	320.	.1	Ni
^{52}Mn	5.63	744.2	.90	Co,Ni
		935.	.94	
		1434.3	.99	
^{52}Fe	.34479	168.9	.99	
^{54}Mn	312.2	834.8	1.00	
^{55}Co	.729	477.	.203	Co,Ni
		931.	.750	
		1408.	.165	
^{56}Co	78.76	846.8	1.00	Co,Ni
^{56}Ni	6.1	159.	.988	Co,Ni
^{57}Co	271.7	122.	.856	Co,Ni
^{57}Ni	1.5	1377.	.776	Co,Ni
^{58}Co	70.78	811.	.994	Co,Ni
^{60}Co	1925.	1173.	.999	Co
		1132.	.999	
^{65}Ni	.105	366.3	.0461	Ni
		1115.3	.148	
		1481.7	.235	

Table I-2(b)

Nuclear Data used in the Evaluation of Cross Sections for Indium.

Nuclide	Half-life (days)	E_γ (keV)	I_γ (%)
^{114m}In	49.51	190.2	.156
^{114m}In		558.2	.0465
^{114m}In		725.2	.033
^{111}In	2.83	245.5	.942
^{115}Cd	2.23	336.2	.501
^{111}Ag	7.45	342.1	.048
^{105}Ag	41.29	280.4	.32
^{105}Ag		344.7	.42
^{106}Ag	8.5	450.5	.284
^{106}Ag		615.8	.217
^{106}Ag		718	.291
^{106}Ag		749.1	.207
^{106}Ag		1199.8	.113

Table I-2(c)

Nuclear Data used in the Evaluation of Cross Sections for Tantalum.

Nuclide	Half-life (days)	E_γ (keV)	I_γ (%)
^{165}Tm	1.252	242.9	.35
		296.0	.23
^{166}Ho	1.117	1379.3	.0093
^{167}Tm	9.24	207.8	.41
^{169}Lu	1.4192	191.2	.207
		960.6	.235
		1449.8	.0996
		1467.	.0334
^{170}Hf	.667	164.7	.33
		572.9	.18
		620.7	.23
^{171}Lu	8.24	667.4	.0328
		739.8	.03
^{171}Hf	.504	295.6	.52
		347.2	.56
		469.2	.38
		540.2	.13
		662.25	1.00
		1071.8	.56
		1749.2	.109
		2022.6	.12
^{173}Hf	.983	123.7	.83
		139.6	.123
		297.0	.339
		311.2	.1074
^{173}Ta	.1521	172.2	.17
^{176}Ta	8.08	710.5	.052
		1555.1	.039
		1584	.051
		1696.5	.045

Table I-2(c) (Con'd)

Nuclear Data used in the Evaluation of Cross Sections for Tantalum.

Nuclide	Half-life (days)	E_γ (keV)	I_γ (%)
^{177}Ta	2.3567	113.7	.065
^{177}Lu	6.71	113.7	.0983
		207.4	.11
^{178}Ta	.102	213.6	.811
		325.5	.941
		331.7	.318
		426.8	.971
^{179m}Hf	24.8	451.	.65
^{181}Hf	42.4	481.1	.81
^{182}Ta	115.	100.1	.14
		113.7	.0193
		152.44	.0718
		156.4	.0273
		79.4	.0314
		198.3	.0152
		222.1	.0861
		264.1	.0362
		891.92	.00053
		927.99	.0061
		959.74	.00364
		1001.68	.02
		1044.3	2.3E-03
		1113.38	4.4E-03
		1121.2	.347
		1157.58	6.7E-03
		1221.4	.273
		1189	.165
		1231	.1163
		1257.47	.0152
		1273.75	6.67E-03
		1289.17	.014
		1342.72	2.6E-03
		1373	2.3E-03

Table I-3
Relative Cross Sections for ^{55}Co, ^{116m}In, ^{176}Ta, and ^{182}Ta

Radionuclide	E_γ(keV)	σ(mb)	%Δσ
^{55}Co	91.8	11.77	24
	385	29.08	20
	411	17.14	19
	477	15.69	3.1
	803	14.23	15
	931	17.49	1.4
	1316	17.17	4.2
	1370	15.29	8.2
	1408	18.73	2.0
		<17.43>	<1.0>
^{116m}In	138	379b	1.7
	417	230	.9
	819	284	1.4
	1097	254	.8
	1293.5	267	.5
	1507.6	248	2.2
	1752.4	290	5.0
	2112	248	1.8
		<261>	<3.4>
^{176}Ta	710.5	1402mb	4.8
	1357.5	1411	5.8
	1555.1	1217	7.7
	1584	1423	4.1
	1616.2	1496	7.4
	1696.5	1282	4.7
	1721.5	1592	5.7
	1823.7	1302	6.7
	1862.5	1400	5.5
		<1383>	<1.8>

Table I-3(con'd)
Relative Cross Sections for ^{55}Co, ^{116m}In, ^{176}Ta, and ^{182}Ta

Radionuclide	E_γ(keV)	σ(mb)	$\%\Delta\sigma$
^{182}Ta	100.1	543b	.6
	152.4	520	1.6
	156.4	523	3.4
	179.4	543	2.9
	198.3	702	4.6
	222.1	515	1.6
	264.1	479	1.8
	1001.7	592	.5
	1121	508	.7
	1189	509	.5
	1221	504	1.3
	1231	480	1.5
	1257.5	492	1.2
	1289.2	521	1.2
		<527.5>	<25>

Table I-4
Quasithermal Neutron Flux

Sample	Flux (10^6 neutrons/sec/cm^2)
Cobalt	1.54
Indium	.27
Tantalum	3.89

Table I-5
Cross Sections(mb) for n-induced reactions on Vanadium

	First		Second		Weighted	
nuclide	σ	%Δσ	σ	%Δσ	σ	%Δσ
^{42}K	14.1	12	10.7	12	11.9	8.6
^{43}Sc	19.4	5.5				
^{43}K	7.9	4.8	6.6	3.8	7.0	3.0
^{44}Sc			203	1.1		
^{44m}Sc	21.6	2.7	20.6	2.6	21.1	1.9
^{46}Sc	128	10.9	85	6.1	90	5.4
^{47}Sc	44.0	4.4	49.1	1.7	48.3	1.6
^{48}Sc	15.3	6.7	15.7	3.1	15.6	2.8
^{48}Cr	1.14	17	.68	25	.88	15
^{48}V	53.2	26	48.9	11	49.5	10

Table I-6
Cross Sections(mb) for n-induced reactions on Cobalt

	First		Second		Weighted	
nuclide	σ	%Δσ	σ	%Δσ	σ	%Δσ
^{44}Sc	1.91	17	2.34	10.2	2.2	8.8
^{44m}Sc	2.36	14.5				
^{46}Sc	60.1	19.4	24.4	19	33	13
^{48}V	12.3	14	12.8	2.8	12.8	2.7
^{51}Cr			57.6	13.3		
^{52}Fe			92	77		
^{52}Mn	18.9	3.4	18.5	4.3	19.2	.4
^{54}Mn	130	10.8				
^{55}Co	5.10	7.3	6.04	6	5.6	4.7
^{56}Mn	19.0	8.1				
^{56}Co	43.9	6.6				
^{56}Ni	3.9	17.5	3.2	7.5	3.3	6.9
^{57}Co	246	19	160	9.1	168	8.3
^{57}Ni	2.2	13	2.7	4.8	2.6	4.5
^{58}Co	293	4.5	315	1.6	312	1.5

Table I-7
Cross Sections(mb) for n-induced reactions on Nickel

	First		Second		Weighted	
nuclide	σ	%Δσ	σ	%Δσ	σ	%Δσ
^{44}Sc	1.81	23	4.65	5.6	3.85	5.7
^{44m}Sc			1.99	7.8		
^{46}Sc			29.5	3.7		
^{48}Sc			.4	14		
^{48}Cr	1.28	21	.80	8.0	.83	7.6
^{48}V	12.0	21	11.3	2.7	11.3	2.7
^{52}Fe	2.12	6.7	2.02	2.7	2.03	2.5
^{52}Mn	14.3	9.8	17.0	1.2	16.9	1.2
^{54}Mn	78	10.5				
^{55}Co	15.4	3.8	17.5	1.1	17.3	1.1
^{56}Mn						
^{56}Co			67	4.5		
^{56}Ni	3.2	31	5.2	3.3	5.14	3.3
^{57}Co						
^{57}Ni	45.1	2.8	44.5	.6	44.5	.6
^{58}Co	181	8.4	228	1.3	226	1.

Table I-8
Cross Sections for n-produced reactions on Indium

nuclide	σ(mb)	%Δσ
^{105}Ag	50.7	12.3
^{106}Ag	22.07	6.5
^{111}In	131	1.0
^{115}Cd	4.5	18
^{115m}In	260	15

Table I-9
Cross Sections for n-produced reactions on Tantalum

nuclide	σ(mb)	%Δσ	E_γ(keV) used
165Tm	12	32	243
166Ho	90	43	1379
167Tm	*		
169Lu	90	4.3	1450,1467
170Hf	95	2.0	165,573,621
171Lu	53.9	11.4	740
171Hf	16.5	2.1	469,662 1072,2023
173Hf	185	4.1	311
173Ta	145	20	172
176Ta	1383	1.8	711,1555,1584
177Lu	*		
177Ta	*		
178Ta	67	1.0	214,326,332,427
179mHf	70	20	451
181Hf	245	11	481

* No results are given because contributions from 113 and 208 keV peaks could not be separated.

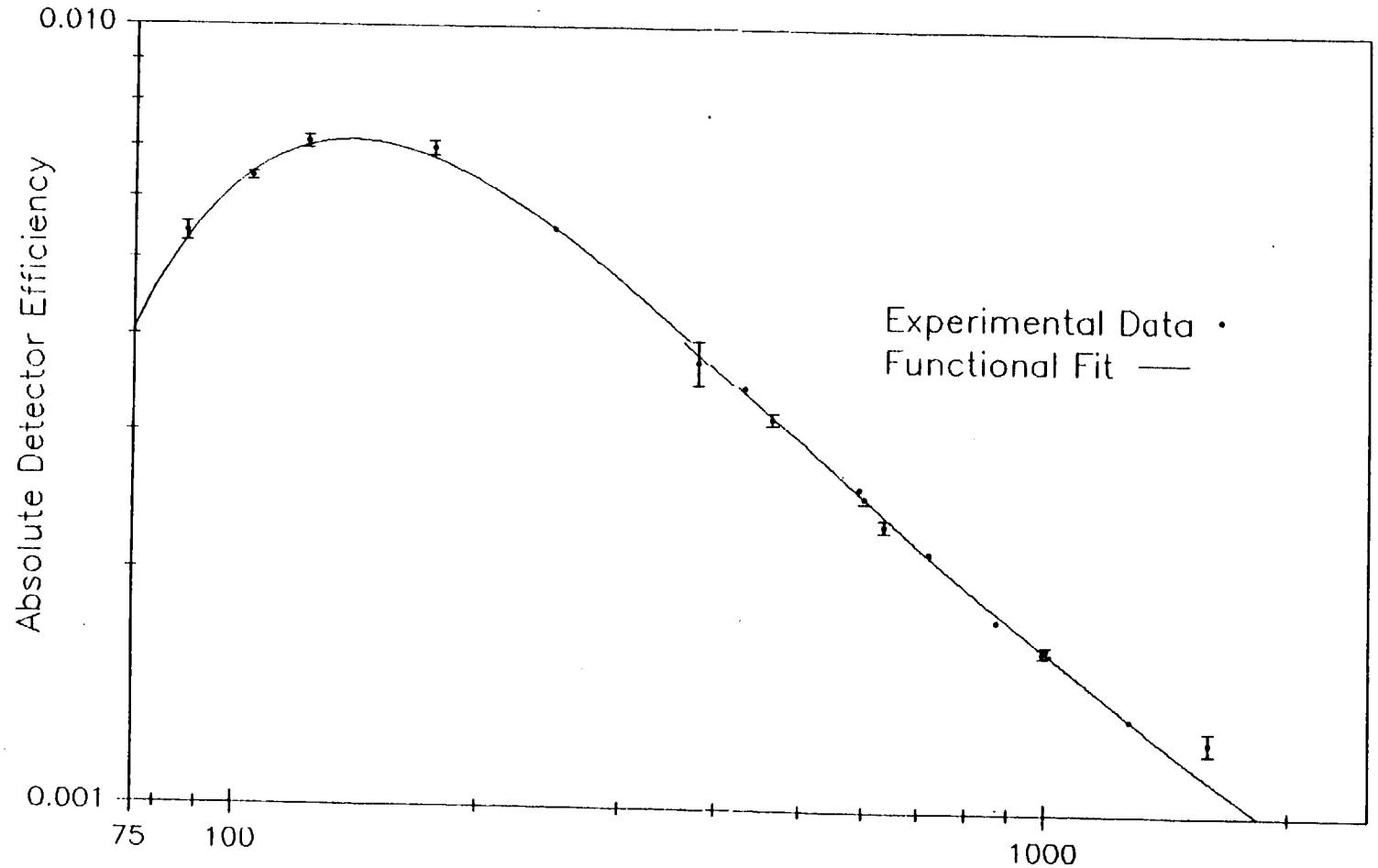

Figure I–1 Efficiency of IUCF Detector at 10cm.

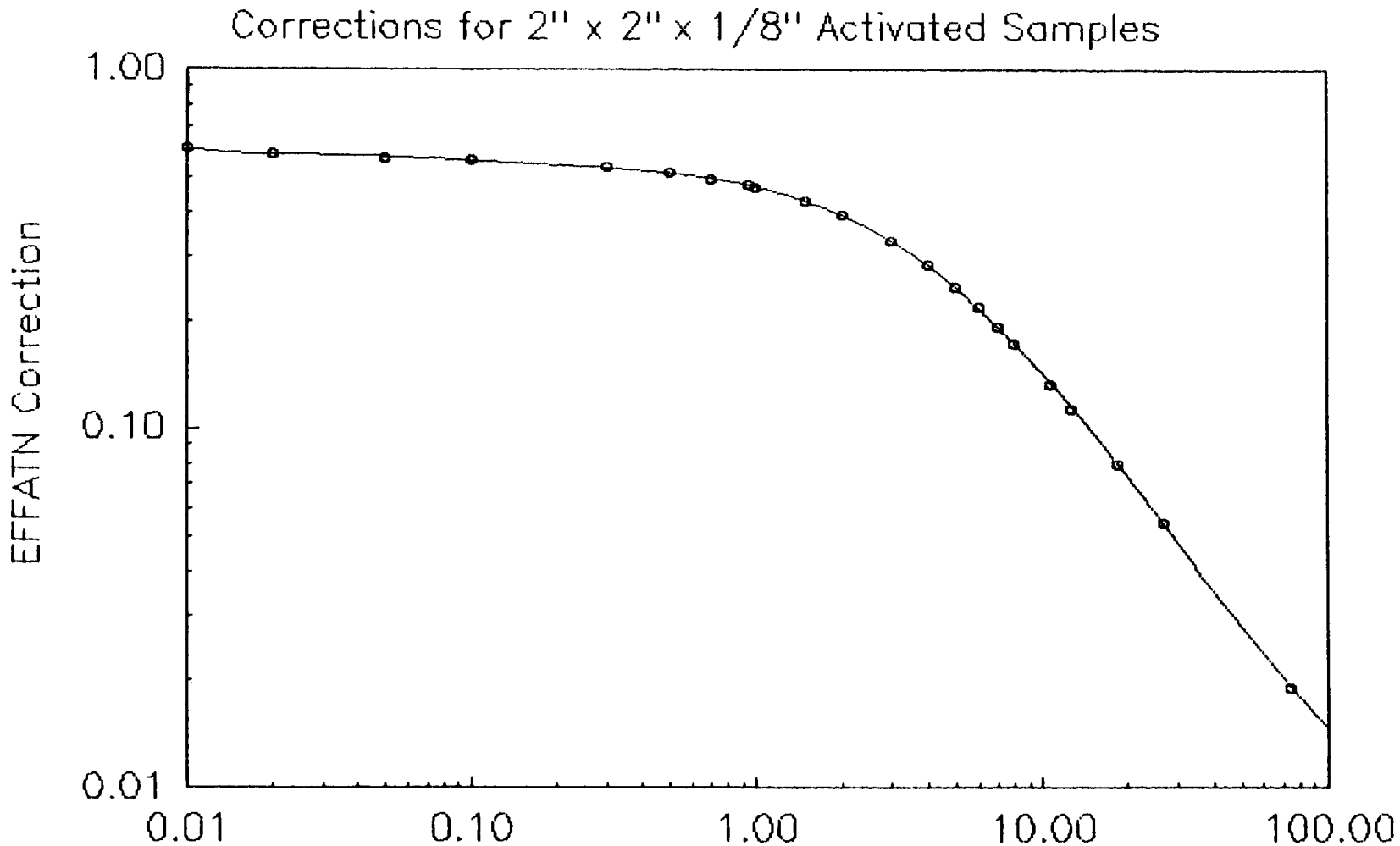

Figure I-2 Corrections for IUCF Experiment

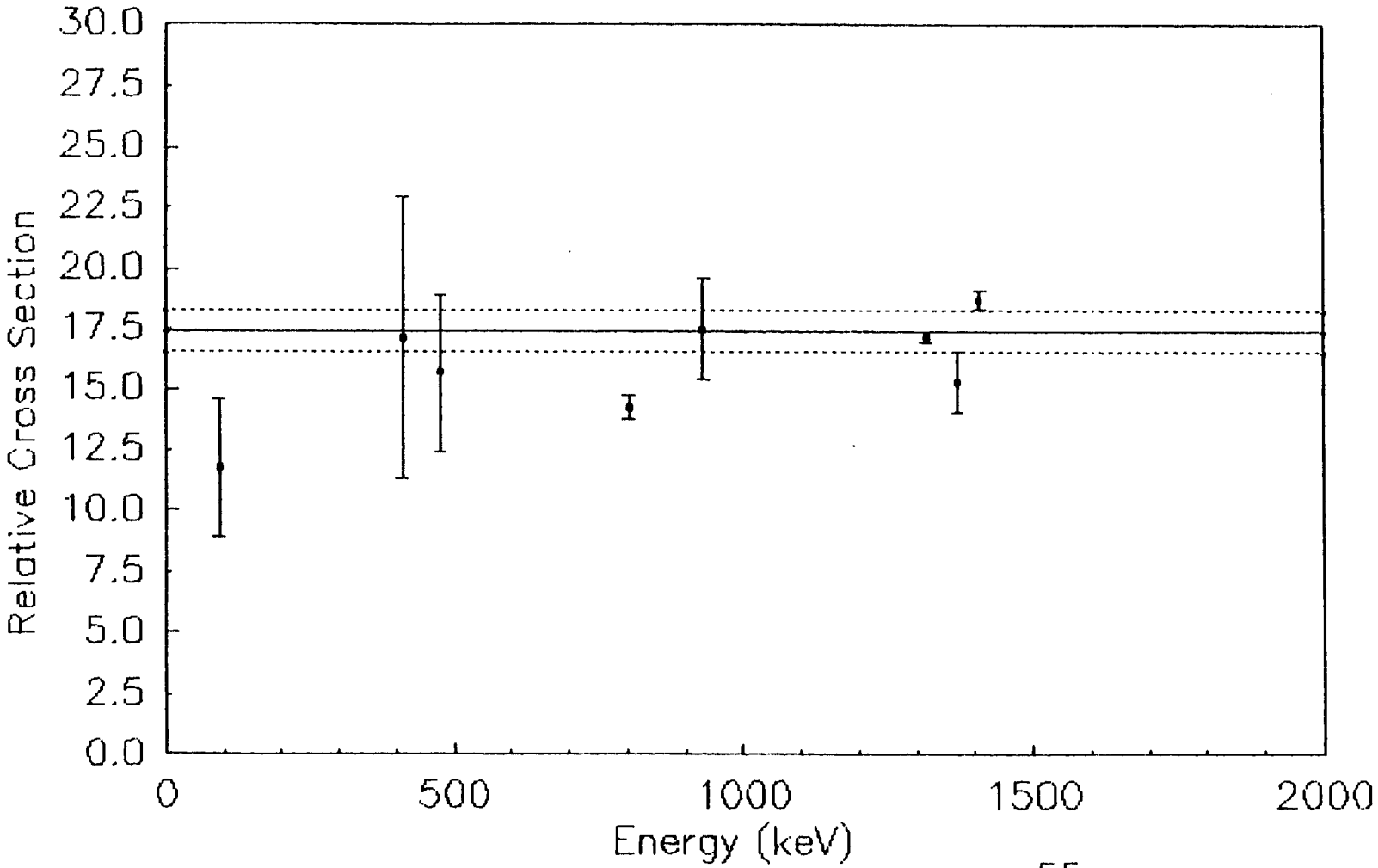

Figure I-3(b) Relative Cross Section for ^{55}Co
(The lines are the weighted average +/- 5%)

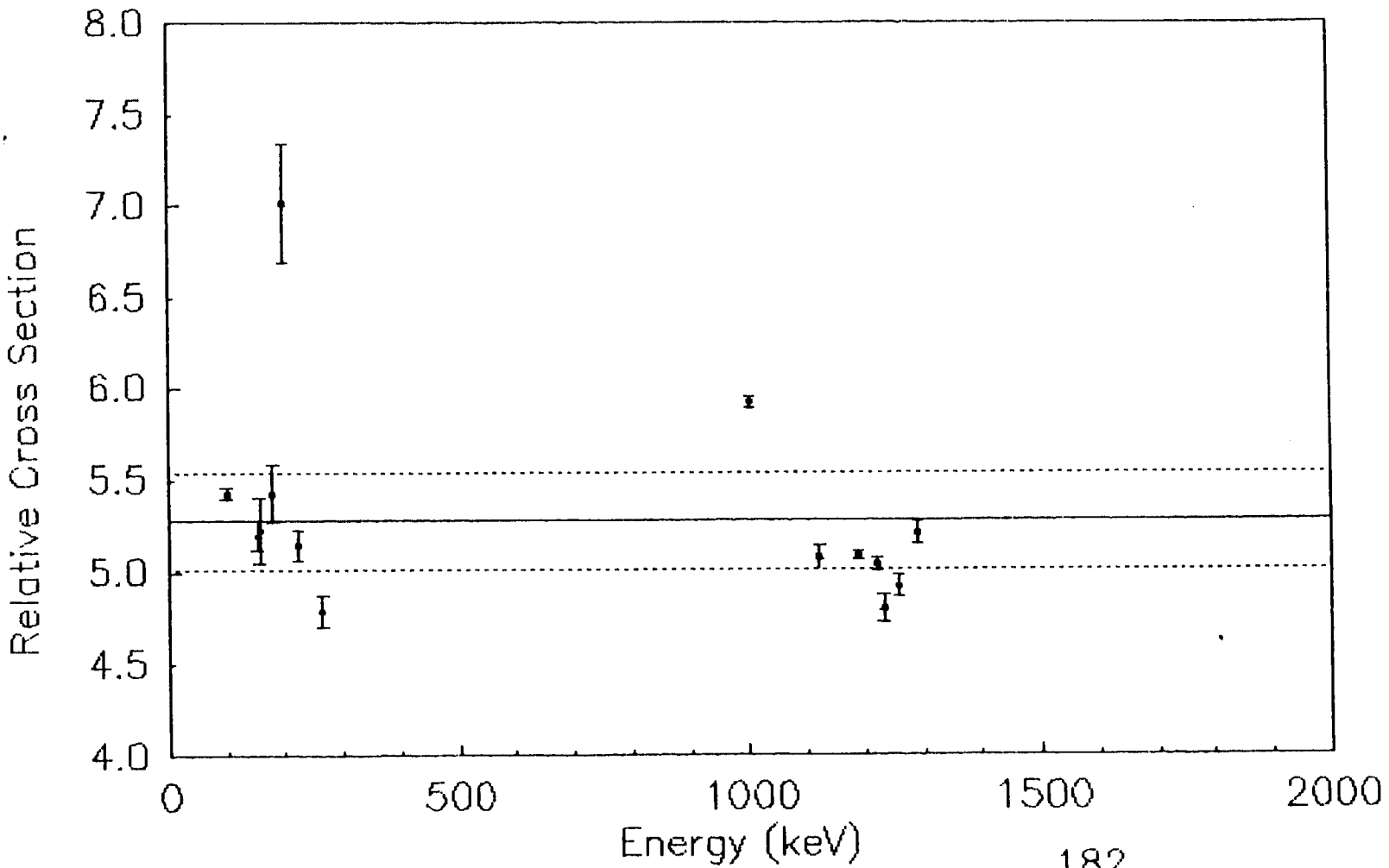

Figure I–3(a) Relative Cross Section for ^{182}Ta
(The lines are the weighted average +/– 5%)

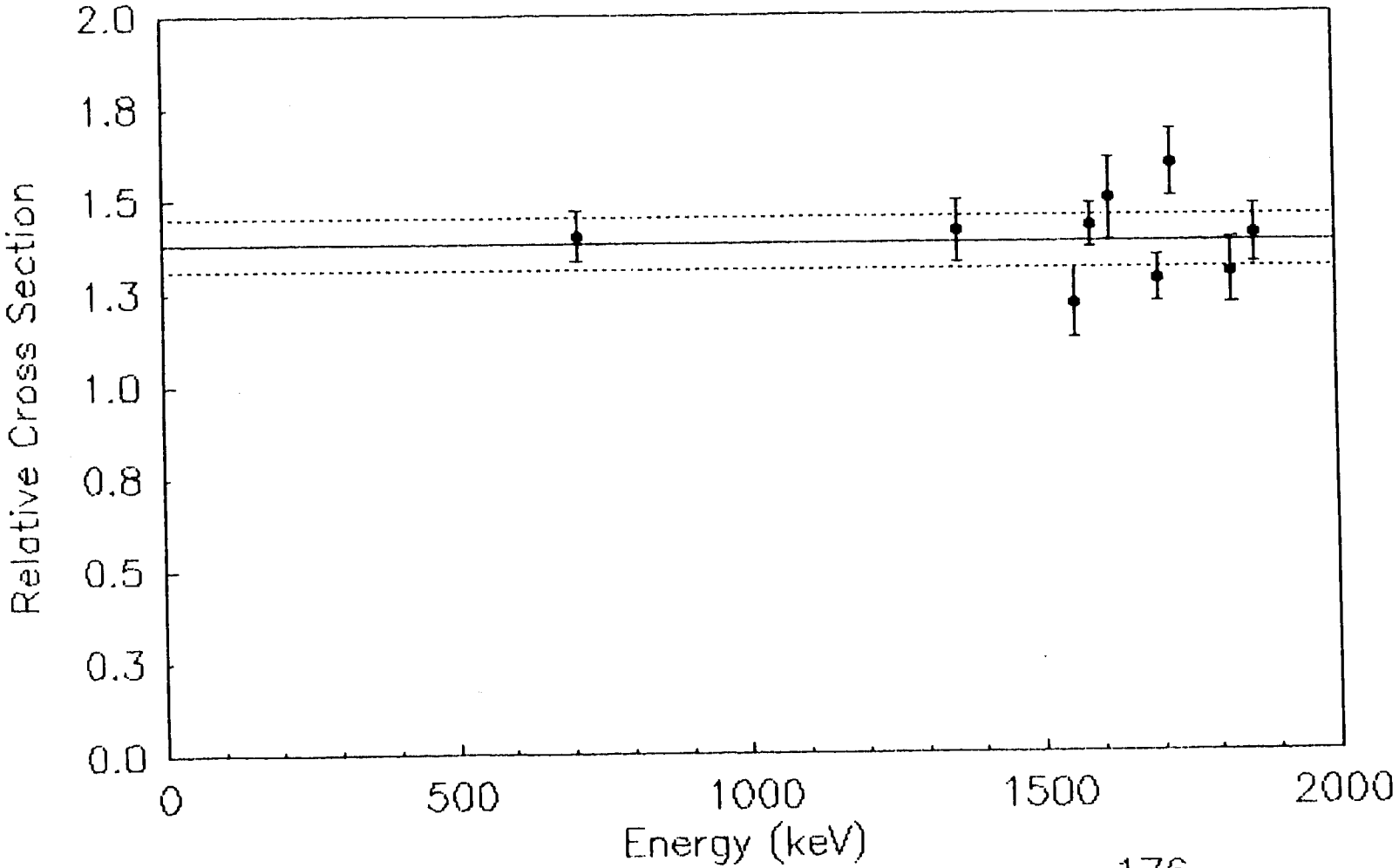

Figure 1-3(c) Relative Cross Sections from ^{176}Ta
(The lines are the weighted average +/- 5%)

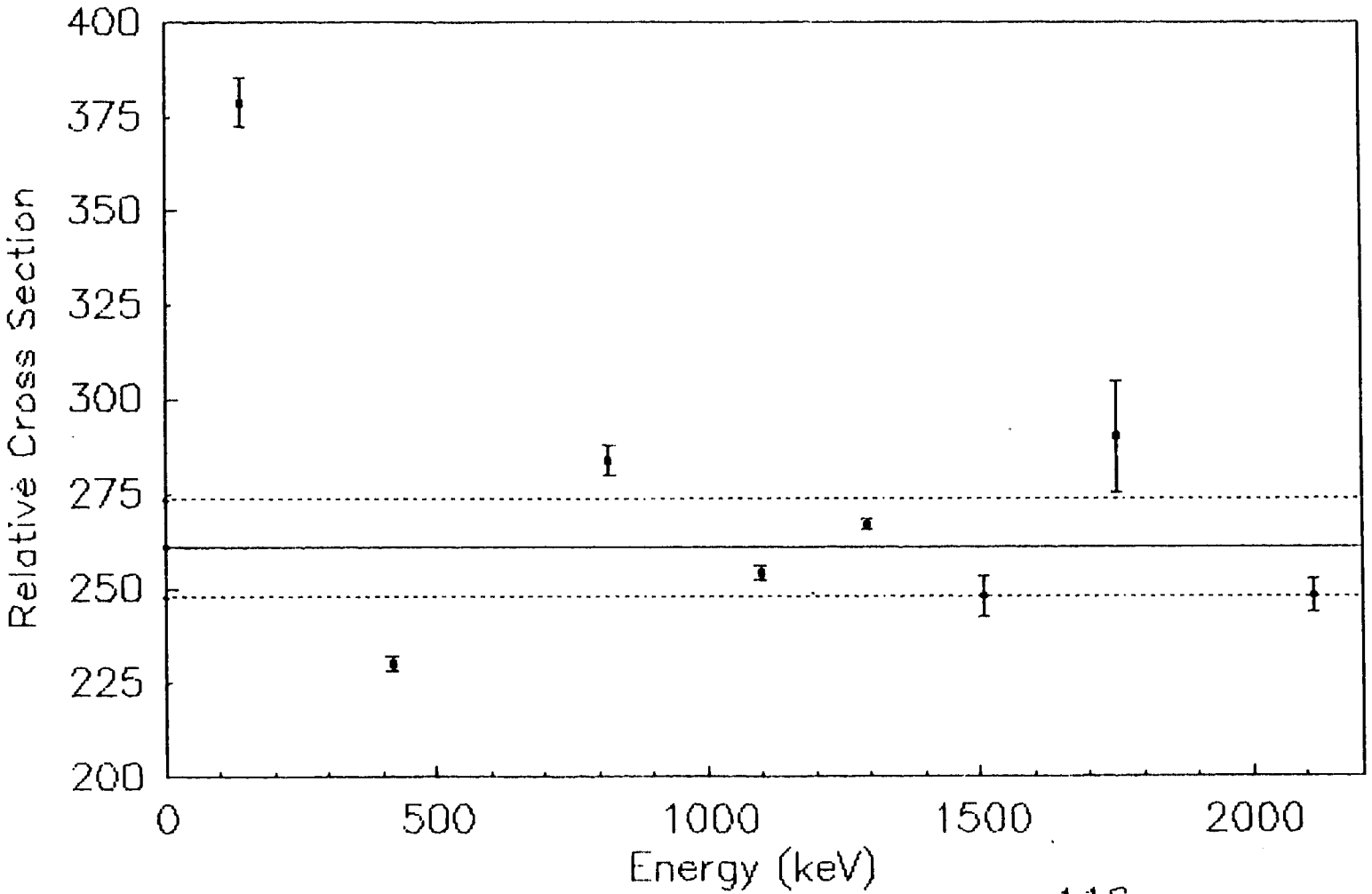

Figure 1-3(d) Relative Cross Section for ^{116m}In
(The lines are the weighted average +/- 5%)

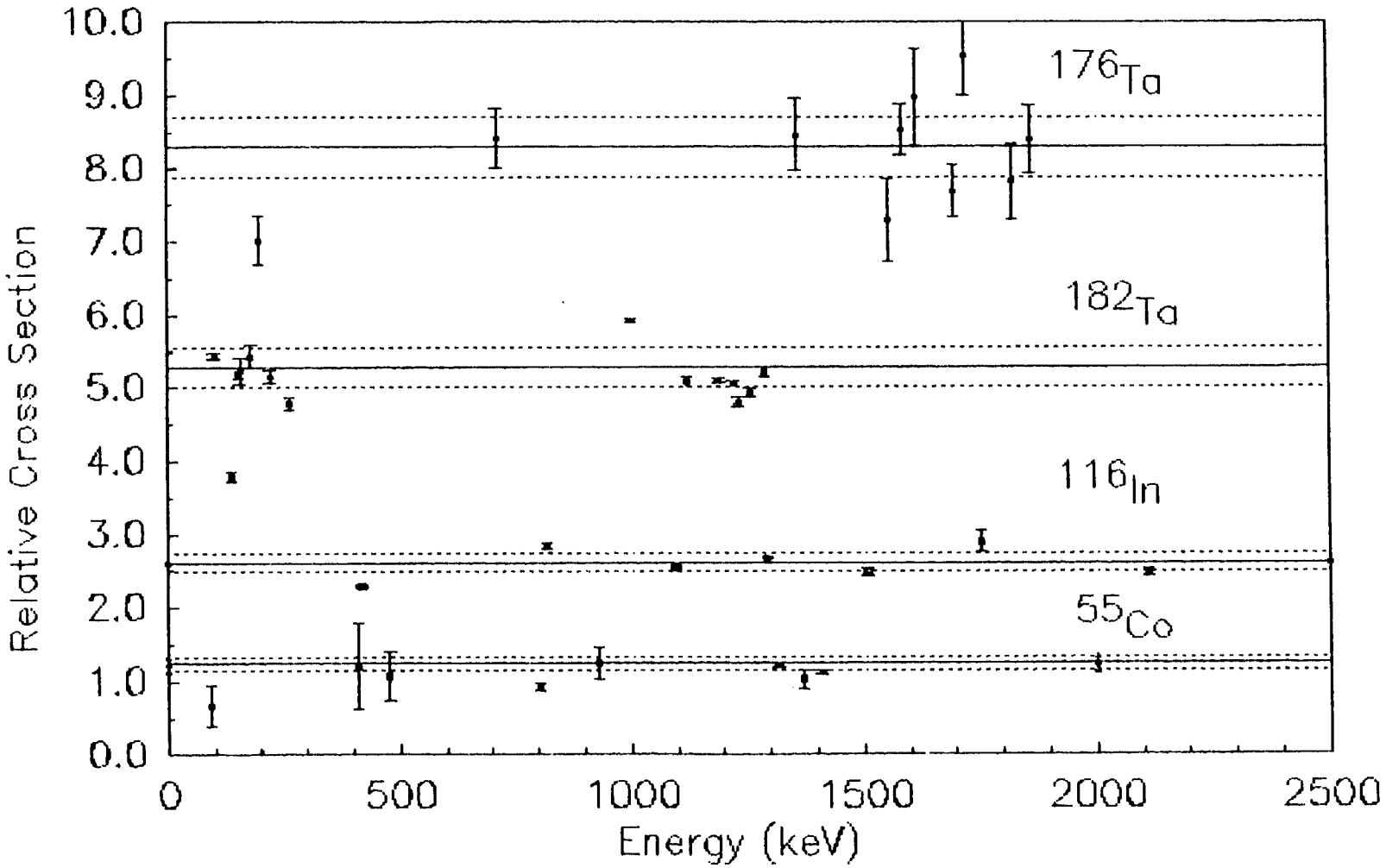

Figure 1-3(e) Comparison of the Results for the Four Nuclides.

SECTION II

Updated Compilation of Activation Cross Sections

In addition to the intentional samples (V, Ni, Co, In, & Ta) flown aboard LDEF and detailed in a previous technical report[1], several other metallic samples have been made available. Included among these are titanium, aluminum, and stainless steel. Since the stainless steel samples are approximately 75% iron and 15% chromium, knowledge of chromium reaction cross sections is also needed. However, no experimental cross sections for chromium have yet been found.

The cross-section literature search for reaction cross sections given in the previous report was terminated as of about January 1, 1984. Subsequent to that date several publications by Michel, et al.[2] greatly contributed to the reaction data available, to the energy range of the studies, and to the overall reliability of the data. Included in the computer code PTRAP4 results in Section III are the additional activation cross sections relevant to this project. Reference (3) gives activation cross sections on V, Mn and Co from 45 to 200 MeV for incident protons. In the region of overlap cross sections for Co agree well with these published by Schoen et al.[4]. Also, there is good agreement with the experimental measurements reported by this author in ref. (1) except for ^{48}V. The reason for this problem may be the confusion over branching ratios for ^{48}Sc and ^{48}V mentioned in the Section I.

Reference (2) gives Ti, Fe and Ni activation cross sections for proton energies from 75 to 200 MeV. The activation cross sections for nickel from 12 to 45 MeV were tabulated in the previous report[1] while those for iron and titanium are given in references (5) and (6), respectively. Unfortunately, the data for the these targets from 45 to 75 MeV, which has been published[7] is not currently available to this investigator. This energy gap is partially filled for iron with data from the work by Williams and Fulner[8]. Their data for ^{52}Mn and ^{54}Mn for energies of 38 to 56 MeV have been incorporated in this study.

Included in the data from Ref.(2) is a compilation of cross sections for proton reactions on aluminum producing ^{22}Na and ^{24}Na.. Since several unintentional samples are aluminum, these were included in our compilation. The ^{22}Na data is an interpolation from

other data[9]. The ^{24}Na data are those obtained by Michel which agree with Ref. (9).

Additional activation cross sections for iron and titanium have been done by Brodzinski, Rancitelli, Cooper, and Wogman[10,11] for proton energies from 14 to 585 MeV. These results usually agree to within two standard errors with Michel, et al. and are measured at fewer energies for the region less than 200 MeV. The data above 200 MeV is useful in estimating activation at higher energies.

The observation of a strong ^{54}Mn signal (E_γ = 835 keV) in the Ni samples dictates the need for accurate cross sections for the production of this isotope. The gap in the tabulated cross section from 56 to 78 MeV may significantly effect the activation calculations. Proton-induced reactions on Co show a large peak cross section within 30 MeV of the reaction threshold. The ^{54}Mn production cross section may peak in the 56 to 77 MeV region in such a way that it could significantly increase activation calculations. Additional data for this reaction should be obtained for the energy region of interest.

References for Section II

1. C. E. Laird, Study of Proton and Neutron Activation of Metal Samples in Low-Earth Orbit, July, 1985, Final Technical Report, NASA Contract NAS8-35180.

2. R. Michel and R. Struck, J. Geophysical Research, **89**(Supplement), B673(1984).

3. R. Michel, F. Peiffer, and R. Stuck, Nucl. Phys. A**441**, 617(1985).

4. N. C. Schoen, G. Orlov, and R. J. McDonald, Phys. Rev. C**29**, 88(1979).

5. R. Michel, G. Brinkmann, H. Wiegel and W. Herr, Nucl. Phys. A**322**, 40(1979).

6. R. Michel, G. Brinkmann, H. Wiegel and W. Herr, J. Inorg. Nucl. Chem. **40**, 1845(1978).

7. R. Michel, F. Peiffer and R. Stuck, in Progress report on nuclear data research in the Federal Republic of Germany, for the period

April 1, 1983 to March 31, 1984, NEANDC(E)-252 U vol. V, INDC(Ger)-27/L+Special, (1984) p.32.

8. I. R. Williams and C. B. Fulmer, Phys. Rev. **162**, 1055(1967).

9. J. Tobailem and C. H. de Lassus St. Genies, report CEA-N-1466(3) (1975).

10. R. L. Brodzinski, L. A. Rancitelli, J. A. Cooper, and N. A. Wogner, Phys. Rev. C**4**, 1250(1971).

11. R. L. Brodzinski, L. A. Rancitelli, J. A. Cooper, and N. A. Wogner, Phys. Rev. C**4**, 1257(1971).

SECTION III

Predicted Activation of LDEF Material

The Appendix contains the results of activation calculations for aluminum, titanium and iron as well as a modification for the previously reported results for nickel.[1] These calculations were done with PTRAP4, a modification of IRTRAP,[1] and are for normal incidence and uniform incidence with and without 5 gram/cm^2 of aluminum covering material(except for nickel where 2.57 g/cm^2 to be consisted with previous calculations). For the sake of consistancy the flux of activating protons are those from the previous report.[1] These results can be scaled to the the flux appropriate to the satellite retrieval as has been stated by Watts.[2] These fluxes used here are appropriate for the original proposed LDEF orbit of 300 nautical miles, 30^o inclination.[3] Since the satellite was in orbit for six years, was placed in orbit near a period of minimum solar activity(and, thus a higher trapped proton flux), was retrieved during a solar minimum, and was in a rapidly decaying orbit upon retrieval, these fluxes are too high by a factor of from 2.88 to 10.8 depending on the assumption of a 250 nm solar min flux or of a 200 nm solar max flux.[4]

Alan Harmon[4] has compared the calculations from Ref.(1) for nickel and has found general agreement. Similar comparisons have not been done for the other "intentional" samples nor for the "unintentional" since the counting process is not yet complete.

In principle, the activation calculation should be done using physical parameters closer to the LDEF environment. These include:

1. specifying the covering material for each specimen,

2. considering the omnidirectional nature of the trapped proton flux, and

3. considering the activation as a function of the orbit of LDEF which was decaying rapidly over the last few months of its mission.

Items (1) and (2) have been studied by Armstrong and Colborn,[5] but an independent calculation using the PTRAP code should be made. Item (3) can be achieved by specifying the proton flux as a function of the time in orbit proceeding backwards in time from the date of

retreival. At each time considered(perhaps day) the activation for the appropriate flux can be calculated and the decay to date of retreival calculated. Doing this for three half-lives of each radioisotope produced or to the date of orbital insertion should yield a more accurate activation for comparison.

References for Section III

1. C. E. Laird, Study of Proton and Neutron Activation of Metal Samples in Low-Earth Orbit, July, 1985, Final Technical Report, NASA Contract NAS8-35180.

2. J. W. Watts, "LDEF Dose Predictions and Measurements", LDEF Ionizing Radiation Special Investigation Group Meeting, NASA/MSFC, July, 1990.

3. C. E. Laird, "Studies of Neutron and Proton Nuclear Activation in Low-Earth Orbit", NASA CR-162051, August, 1982.

4. Alan Harmon, Space Science Laboratory, Marshall Space Flight Center, private communication(based on data from reference (2)).

5. T. W. Armstrong and B. L. Colburn, Report No. SAIC-90/1462, Science Applications International Corporation, NASA contract NAS8-38427, September, 1990.

Table III-1. Trapped Proton Activation for Energies below 200 MeV. (Nuclei/Day)

Aluminum Product	With Covering		Without Covering	
	Normal Incidence	Averaged Incidence	Normal Incidence	Averaged Incidence
24Na	49380	50160	77020	67380
22Na	114400	109500	180100	156700
7Be	2944	3030	4779	3895

Table III-1(con'd.)
Trapped Proton Activation for Energies below 200 MeV.
(Nuclei/Day)

Iron Product	With Covering		Without Covering	
	Normal Incidence	Averaged Incidence	Normal Incidence	Averaged Incidence
57Co	6492	4568	10330	14660
56Co	47800	36370	57750	84510
55Co	22810	16920	23840	35420
54Mn	206700	200800	206700	310600
52Fe	7878	8486	7878	11330
52Mn	61480	62190	61570	92650
51Cr	169900	175900	170000	254200
48V	29090	32220	29090	42820

Nickel Product	With Covering		Without Covering	
	Normal Incidence	Averaged Incidence	Normal Incidence	Averaged Incidence
54Mn	27770	36910	43310	80370
58Co	62630	78820	101100	183400
60Co	2916	3753	4677	8520
52Mn	19410	25980	30350	56130
56Ni	10140	12810	16240	29610
57Ni	113400	137700	189900	336100
55Co	39680	51220	63560	115800
56Co	150500	188800	243300	441100
57Co	179800	213100	311100	539900

Titanium Product	With Covering		Without Covering	
	Normal Incidence	Averaged Incidence	Normal Incidence	Averaged Incidence
48V	46350	31760	171100	326200
47Sc	80760	76490	82610	181700
46Sc	164100	149200	165700	364600
44Sc	58210	53840	59030	130100
43Sc	284200	35210	285700	618900

SECTION IV

Corrections for Activation Measurements

Gamma rays detected from thick samples placed in close proximity to Ge(Li) or HPGe detectors must be corrected for detector efficiency, inverse-square effects, and self absorption. The detector efficiency is a function of the position of a point gamma relative to the detector, the size and shape of the detector and any covering material. The self absorption of the sample is dependent on the linear absorption coefficient of the material, which is energy dependent, and on the distribution of radioactive material throughout the sample. The linear absorption coefficients can be obtained from the mass absorption coefficients[1], the atomic masses[2], and the sample density[2]. The efficiency of the detector for a point source on the detector axis can usually be accurately represented by the function

$$\ln \varepsilon = a/E_\gamma + b + c \ln(E_\gamma) + d(\ln E_\gamma)^2 + e(\ln E_\gamma)^3 \qquad \text{(IV-1)}$$

where ε is the detector efficiency and E_γ is the gamma ray. The efficiency can readily be obtained from gamma-ray spectra of calibrated mixed gamma-ray obtained sources or multiple gamma-ray emitting isotope like ^{152}Eu along with the acquisition live time. A nonlinear least squares fit of such data to the equation above usually yields excellent agreement to the data. This has already been discussed in Section I.

Corrections for off-axis points may be modeled using the on-axis efficiency and an assumed inverse square effect. Careful study of the on-and-off axis efficiency can be made at various distances from the detector and fit to a model. Such a procedure was described in Section I. A similar procedure was followed to determine inverse-square and self-attenuation effects for the low background counting facility at the Space Science Laboratory.

This model has been used to calculate this correction using the program EFFATN developed as part of this NASA funded project. Tables(IV-1) and Figure(IV-1) give the corrections for 2" x 2" x .125", 2" x 2" x. .25", 2" x 1" x .125", 2" x 1" x .25", 1.55" x 2.04" x .3937" parallelopipeds and for coaxial cylinders with inner diameter 1.625", outer diameter 3.23" and thicknesses of 1" and .5" as well as

a 1" thick solid cylinder with the same radius. These corrections assume that the efficiency has been measured(or averaged) over the surface of the detector housing. Preliminary results of these calculations have been reported to the Space Science Laboratory(SSL) at MSFC. Other dimensions of the same shapes can readily be calculated with EFFATN.

Table (IV-2) contains the linear absorption coefficients(μ) for a large number of materials including the intentional samples as well as several the intentional samples such as iron(Fe), manganese(Mn), stainless steel(Ss), and aluminum(Al). The stainless steel was assumed to contain 15.7% Cr, 3.6% Cu, 74.5% Fe, and 4.5% Ni by weight. The tabulated stainless steel linear absorption coefficients were calculated assuming these fractional weights to obtain the appropriate fractional atomic abundances using

$$\mu = \Sigma_i \, f_i \, N_A \, \sigma_i \, \rho_i / A_i \qquad \text{(IV-2)}$$

where μ is the linear absorption coefficient, σ is the total photon reaction cross section, N_A is Avogadro's number, f_i is the elemental fractional abundance by weight, ρ is the elemental density and A_i is the atomic weight.

As part of the work under this contract, approximately 100 gamma-ray spectra from SSL were analyzed to determined the photopeak activity using the IBM 3090 based program SAMPO[3] or the IBM PC based program Peakarea. The results of the peak analyses have already been reported to SSL and will not be included in this report. Part of this data consisted of spectra taken with a planar source made by drop evaporating a mixed, gamma-ray solution onto a flat card. Figure (IV-2) at the end of this section gives the surface efficiency of the detector for this source at energies from 88 to 1836 keV and the fit to Eq.(IV-1). The coefficients of the Eq.(IV-1) are

a = 193.2511
b = -46.33519
c = 20.3162
d = -3.106065
e = .1521919.

(A large number of digits are given for these constants for use in calculations because of the danger of serious round-off error for this power series in the natural log of the energy.) The uncertainty in the efficiency data is about 5% or less while values from the fit disagree with the input data by 3% or less. Therefore, the uncertainty in the efficiencies determined are considered to be 5%. However, the upturn of the fit curve above 1836 keV implies that this fit should not be used at these energies because efficiency curves for Ge(Li) detectors at higher energies generally do not turn up.

In addition, the planar source was used to obtain the efficiency through aluminum and stainless steel absorbers of various thicknesses. This data was used to obtain the parameters for the EFFATN. Figure (IV-3) shows the photopeak yields for three of the gamma rays for various thicknesses of stainless steel and the yield predicted by EFFATN. The EFFATN-predicted yield is given by the straight line with the dots being the uncorrected yields. With a possible exception of the 88 keV peak the agreement of the EFFATN-corrected yields is better than 5%.

The various counting facilities, except for Johnson Space Center(JSC), have used their inverse-square and self-absorption correction in their reported results for the samples for which the corrections can be readily made. Materials such as screws can not be analyzed in any reasonable way and so have not been corrected. The groups at JSC and Lawrence Berkeley Laboratory have not, as of December 31, 1990, supplied these corrections for their detector systems. However, ratios of yields for a planar mixed-gamma source placed in front of and behind various samples have been reported by JSC. These ratios are quite similar to the MSFC ratios as indicated in Figure(IV-4) where the data points are the ratios from JSC for the nickel sample and the curve is the correction for the MSFC data for one of the stainless-steel samples. With additional work using the JSC data it seem apparent that EFFATN can be used for correcting their data.

References for Section IV

1. C. M. Davisson and R. D. Evans, Rev. Mod. Phys. **24**, 79(1952)

2. C. E. Laird, Study of Proton and Neutron Activation of Metal Samples in Low-Earth Orbit, July, 1985, Final Technical Report, NASA Contract NAS8-35180.

3. Reference (3) of Section I.

Table IV-1(a)

EFFATN Corrections for Various Samples
(relative to the efficiency of a 2" x 2" planar source)

$\mu(cm^{-1})$	A	B	C	D	E
15	.195	.097	.208	.104	.165
10	.282	.135	.300	.155	.242
5	.469	.275	.497	.292	.422
2	.698	.512	.734	.539	.668
1	.811	.669	.850	.702	.799
.8	.836	.709			
.7		.730	.890	.764	.845
.6	.863	.752			
.5			.918	.810	.878
.4		.799			
.3		.850	.947	.860	.912
.2		.824	.962	.887	
.1		.877	.977	.915	.949
.02	.947	.899			
.01	.949	.902	.991	.928	.977
.005	.950	.904			

A: 2" x 2" x 1/8" parallelopiped
B: 2" x 2" x 1/4" "
C: 2" x 1" x 1/8" "
D: 2" x 1" x 1/4" "
E: .610" x .803 x .155" "

Table IV-1(b)

EFFATN Corrections for Various Samples
(relative to the efficiency of a 2" x 2" planar source)

$\mu(cm^{-1})$	A	B	C
15	.02774	.0265	.0559
10	.04286	.04096	.0840
5	.08545	.08190	.1648
2	.1994	.1920	.3659
1	.3454	.3340	.5618
.8	.3996	.3870	.6210
.6	.4699	.4560	.6903
.5	.5130	.4982	.7292
.3	.6201	.6037	.8173
.2	.6871	.6697	.8671.
.1	.7652	.7468	.9213
.05	.8093	.7904	.9501
.03	.8279	.8087	.9621
.01	.8471	.8278	.9742
.005	.8520	.8327	.9772

A: Solid Cylinder 4.10 cm radius, 2.54 cm thick
B: Cylinder, outer radius 4.10 cm, inner 2.06, 2.54 cm thick
C: Cylinder, outer radius 4.10 cm, inner 2.06, 1.27 cm thick

Table IV-2

Photo-absorption Cross Section (Barns/atom)

E(keV)	Al	Ti	U	Cr
102.2	7.361	21.2	24.14	26.8
127.7	6.518	15.5	17.09	18.9
170.3	5.751	11.5	12.39	13.4
255.4	4.923	8.82	9.38	9.87
340.5	4.401	7.63	8.11	8.44
408.6	4.095	7.02	7.48	7.74
510.8	3.732	6.35	6.75	6.98
681.1	3.29	5.57	5.92	6.11
1022	2.718	4.59	4.87	5.02
1362	2.353	3.97	4.22	4.35
1533	2.214			
2043	1.911	3.26	3.46	3.57
Density	2.7	4.51	6.1	7.19
At.wgt	26.982	47.9	50.94	51.996
	0.0602602	0.0566998	0.0721127	0.0832721

Linear Absorption Coefficients (1/cm)

E(keV)	Al	Ti	U	Cr
102.2	0.4436	1.2020	1.7408	2.2317
127.7	0.3928	0.8788	1.2324	1.5738
170.3	0.3466	0.6520	0.8935	1.1158
255.4	0.2967	0.5001	0.6764	0.8219
340.5	0.2652	0.4326	0.5848	0.7028
408.6	0.2468	0.3980	0.5394	0.6445
510.8	0.2249	0.3600	0.4868	0.5812
681.1	0.1983	0.3158	0.4269	0.5088
1022	0.1638	0.2603	0.3512	0.4180
1362	0.1418	0.2251	0.3043	0.3622
1533	0.1334	0.0000	0.0000	0.0000
2043	0.1152	0.1848	0.2495	0.2973

Table IV-2 cont'd

Photo-absorption Cross Section (Barns/atom)

E(keV)	Mn	Fe	Co	Ni
102.2	30.2	33.28	36.9	41.6
127.7	20.89	22.9	25.5	28.21
170.3	14.43	15.54	16.83	18.15
255.4	10.44	11	11.63	12.26
340.5	8.879	9.306	9.743	10.19
408.6	8.121	8.488	8.863	9.24
510.8	7.313	7.641	7.948	8.27
681.1	6.392	6.658	6.927	7.19
1022	5.253	5.468	5.684	5.89
1362	4.549	4.736	4.92	5.1
1533		4.46		
2043	3.739	3.895	4.051	4.21
Density	7.43	7.86	8.9	8.9
At.wgt	54.94	55.85	58.93	58.71
	0.0814406	0.0847501	0.0909482	0.091289

Linear Absorption Coefficients (1/cm)

E(keV)	Mn	Fe	Co	Ni
102.2	2.4595	2.8205	3.3560	3.7976
127.7	1.7013	1.9408	2.3192	2.5753
170.3	1.1752	1.3170	1.5307	1.6569
255.4	0.8502	0.9323	1.0577	1.1192
340.5	0.7231	0.7887	0.8861	0.9302
408.6	0.6614	0.7194	0.8061	0.8435
510.8	0.5956	0.6476	0.7229	0.7550
681.1	0.5206	0.5643	0.6300	0.6564
1022	0.4278	0.4634	0.5169	0.5377
1362	0.3705	0.4014	0.4475	0.4656
1533	0.0000	0.3780	0.0000	0.0000
2043	0.3045	0.3301	0.3684	0.3843

Table IV-2 cont'd

Photo-absorption Cross Section (Barns/atom)

E(keV)	In	Ta	Pb	Ss
102.2	336	1324	1822	32.9698
127.7	186	730	1023	22.7250
170.3	89.4	357	500	15.4310
255.4	38.8	133	192	10.9357
340.5	25.7	72.8	103.3	9.2509
408.6	20.8	52.6	73.5	8.4400
510.8	17.01	37.6	51.2	7.5958
681.1	13.87	27.21	35.2	6.6217
1022	10.87	19.05	23.45	5.4373
1362	9.31	15.65	18.87	4.7096
1533				3.4030
2043	7.74	12.79	15.19	3.8734
Density	7.31	16.6	11.4	7.8469
At.wgt	114.82	180.95	207.19	55.5324
	0.038339	0.0552447	0.0331342	

Linear Absorption Coefficients (1/cm)

E(keV)	In	Ta	Pb	Ss
102.2	12.8819	73.1439	60.3706	2.8100
127.7	7.1311	40.3286	33.8963	1.9365
170.3	3.4275	19.7223	16.5671	1.3143
255.4	1.4876	7.3475	6.3618	0.9310
340.5	0.9853	4.0218	3.4228	0.7875
408.6	0.7975	2.9059	2.4354	0.7184
510.8	0.6521	2.0772	1.6965	0.6465
681.1	0.5318	1.5032	1.1663	0.5636
1022	0.4167	1.0524	0.7770	0.4628
1362	0.3569	0.8646	0.6252	0.4008
1533	0.0000	0.0000	0.0000	0.2884
2043	0.2967	0.7066	0.5033	0.3297

Photo-absorption Cross Section (Barns/atom)

E(keV)	Al	Tl	U	Cr
102.2	7.361	21.2	24.14	26.8
127.7	6.518	15.5	17.09	18.9
170.3	5.751	11.5	12.39	13.4
255.4	4.923	8.82	9.38	9.87
340.5	4.401	7.63	8.11	8.44
408.6	4.095	7.02	7.48	7.74
510.8	3.732	6.35	6.75	6.98
681.1	3.29	5.57	5.92	6.11
1022	2.718	4.59	4.87	5.02
1362	2.353	3.97	4.22	4.35
1533	2.214			
2043	1.911	3.26	3.46	3.57
Density	2.7	4.51	6.1	7.19
At.wgt	26.982	47.9	50.94	51.996
	0.06026017345	0.05669983299	0.07211268159	0.08327213632

Linear Absorption Coefficients (1/cm)

E(keV)	Al	Tl	U	Cr
102.2	0.4436	1.2020	1.7408	2.2317
127.7	0.3928	0.8788	1.2324	1.5738
170.3	0.3466	0.6520	0.8935	1.1158
255.4	0.2967	0.5001	0.6764	0.8219
340.5	0.2652	0.4326	0.5848	0.7028
408.6	0.2468	0.3980	0.5394	0.6445
510.8	0.2249	0.3600	0.4868	0.5812
681.1	0.1983	0.3158	0.4269	0.5088
1022	0.1638	0.2603	0.3512	0.4180
1362	0.1418	0.2251	0.3043	0.3622
1533	0.1334	0.0000	0.0000	0.0000
2043	0.1152	0.1848	0.2495	0.2973

Photo-absorption Cross Section (Barns/atom)

E(keV)	Mn	Fe	Co	Ni
102.2	30.2	33.28	36.9	41.6
127.7	20.89	22.9	25.5	28.21
170.3	14.43	15.54	16.83	18.15
255.4	10.44	11	11.63	12.26
340.5	8.879	9.306	9.743	10.19
408.6	8.121	8.488	8.863	9.24
510.8	7.313	7.641	7.948	8.27
681.1	6.392	6.658	6.927	7.19
1022	5.253	5.468	5.684	5.89
1362	4.549	4.736	4.92	5.1
1533		4.46		
2043	3.739	3.895	4.051	4.21
Density	7.43	7.86	8.9	8.9
At.wgt	54.94	55.85	58.93	58.71
	0.08144058973	0.08475008057	0.09094824368	0.09128904786

Linear Absorption Coefficients (1/cm)

E(keV)	Mn	Fe	Co	Ni
102.2	2.4595	2.8205	3.3560	3.7976
127.7	1.7013	1.9408	2.3192	2.5753
170.3	1.1752	1.3170	1.5307	1.6569
255.4	0.8502	0.9323	1.0577	1.1192
340.5	0.7231	0.7887	0.8861	0.9302
408.6	0.6614	0.7194	0.8061	0.8435
510.8	0.5956	0.6476	0.7229	0.7550
681.1	0.5206	0.5643	0.6300	0.6564
1022	0.4278	0.4634	0.5169	0.5377
1362	0.3705	0.4014	0.4475	0.4656
1533	0.0000	0.3780	0.0000	0.0000
2043	0.3045	0.3301	0.3684	0.3843

Photo-absorption Cross Section (Barns/atom)

E(keV)	In	Ta	Pb	Ss
102.2	336	1324	1822	32.9698
127.7	186	730	1023	22.7250
170.3	89.4	357	500	15.4310
255.4	38.8	133	192	10.9357
340.5	25.7	72.8	103.3	9.2509
408.6	20.8	52.6	73.5	8.4400
510.8	17.01	37.6	51.2	7.5958
681.1	13.87	27.21	35.2	6.6217
1022	10.87	19.05	23.45	5.4373
1362	9.31	15.65	18.87	4.7096
1533				3.4030
2043	7.74	12.79	15.19	3.8734
Density	7.31	16.6	11.4	7.8469
At.wgt	114.82	180.95	207.19	55.5324
	0.03833898276	0.05524465322	0.03313422462	

Linear Absorption Coefficients (1/cm)

E(keV)	In	Ta	Pb	Ss
102.2	12.8819	73.1439	60.3706	2.8100
127.7	7.1311	40.3286	33.8963	1.9365
170.3	3.4275	19.7223	16.5671	1.3143
255.4	1.4876	7.3475	6.3618	0.9310
340.5	0.9853	4.0218	3.4228	0.7875
408.6	0.7975	2.9059	2.4354	0.7184
510.8	0.6521	2.0772	1.6965	0.6465
681.1	0.5318	1.5032	1.1663	0.5636
1022	0.4167	1.0524	0.7770	0.4628
1362	0.3569	0.8646	0.6252	0.4008
1533	0.0000	0.0000	0.0000	0.2884
2043	0.2967	0.7066	0.5033	0.3297

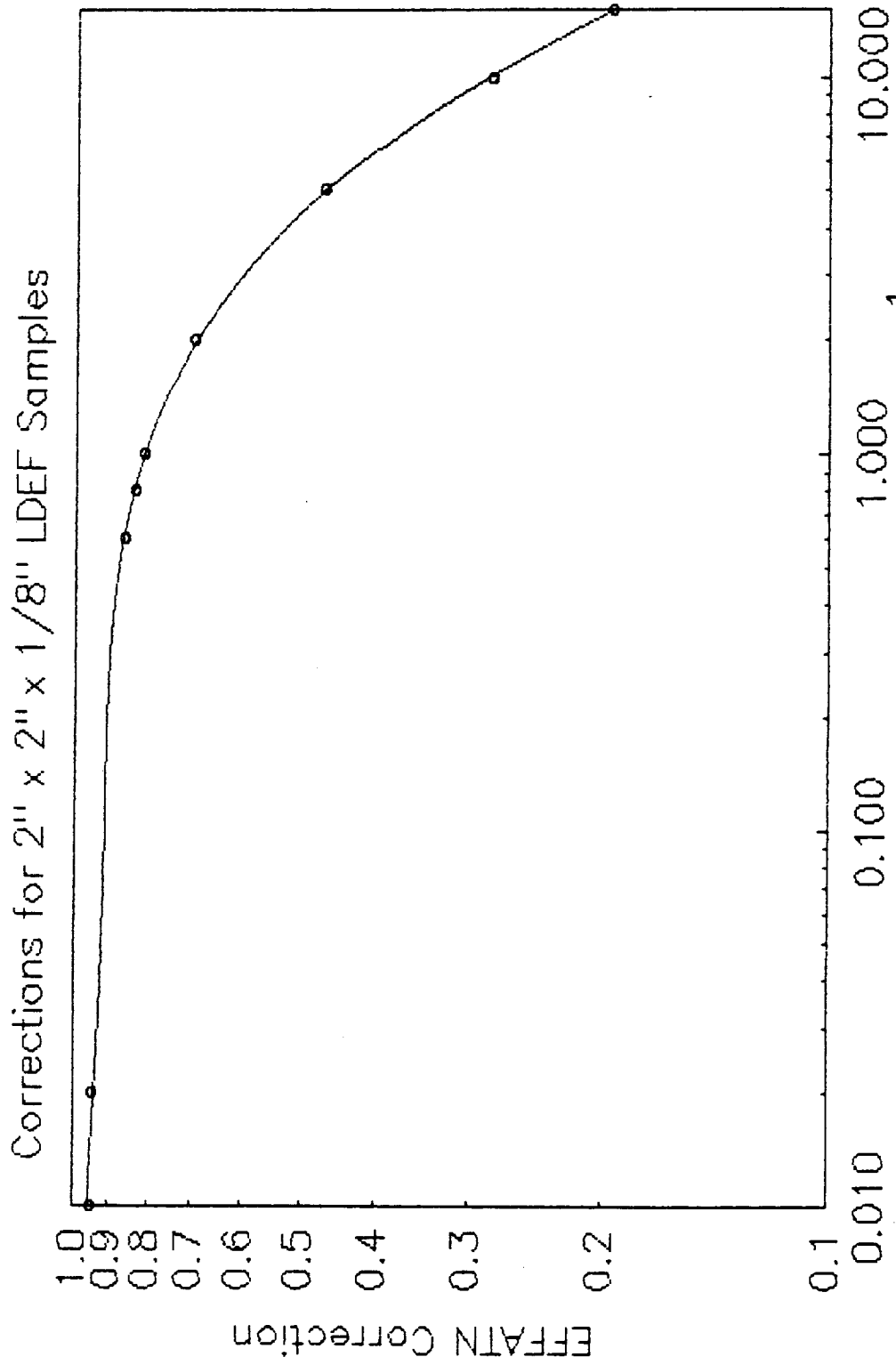

Figure IV–1(a) Correction for 2" x 2" x 1/8" Sample

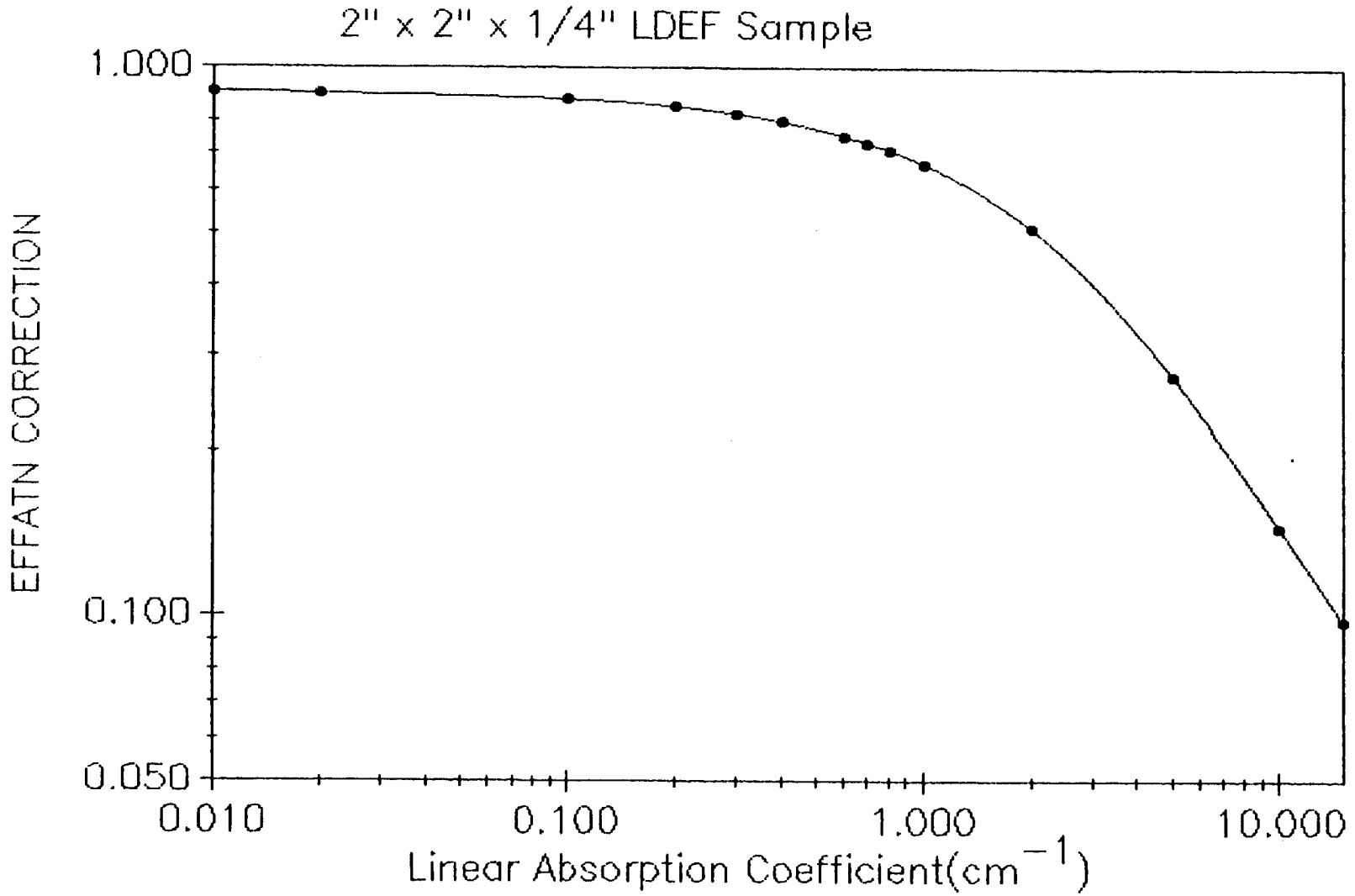

Figure IV–1(b) Correction for 2" x 2" x .25" Sample

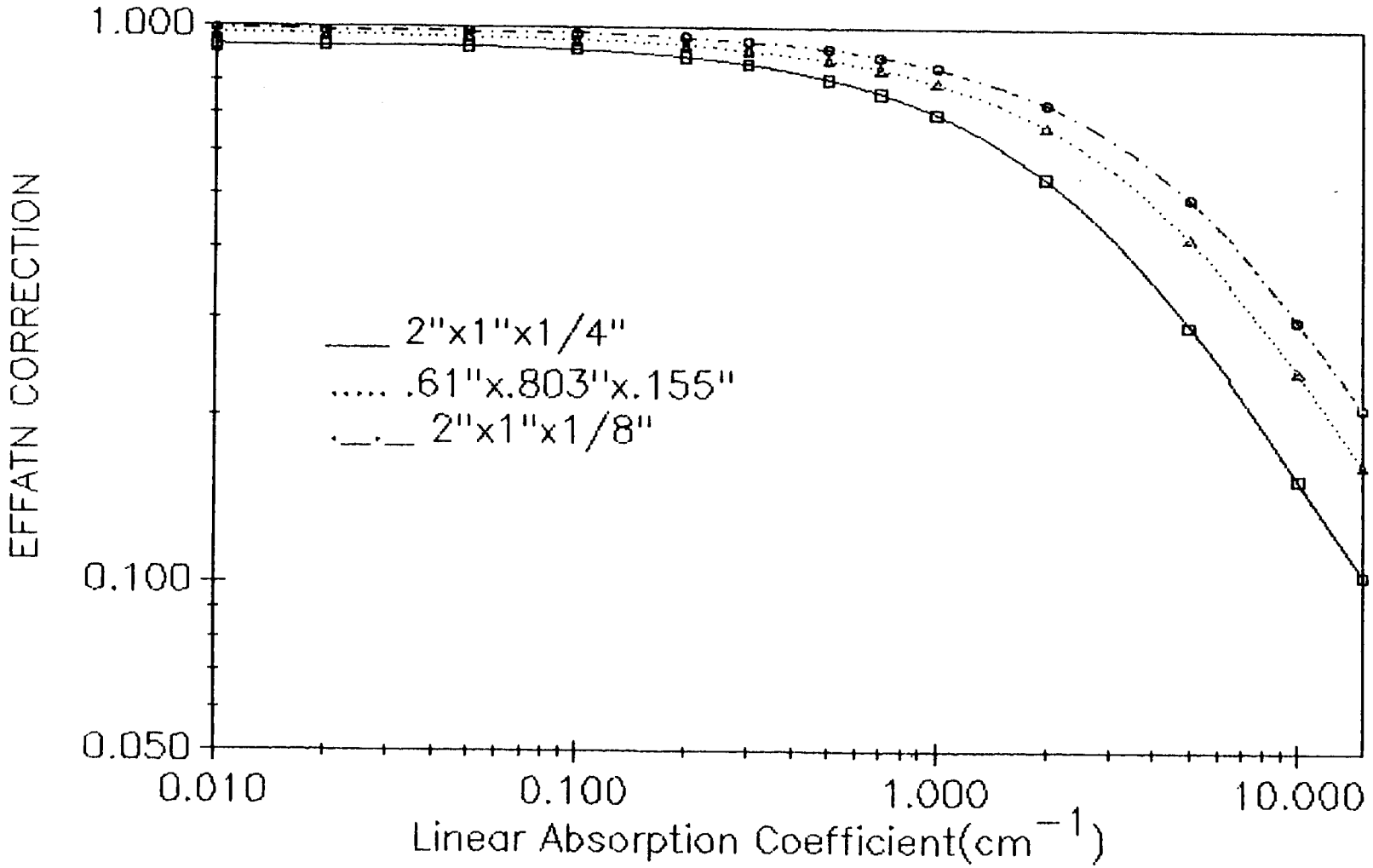

Figure IV-1(c) EFFATN Correction for Three Samples

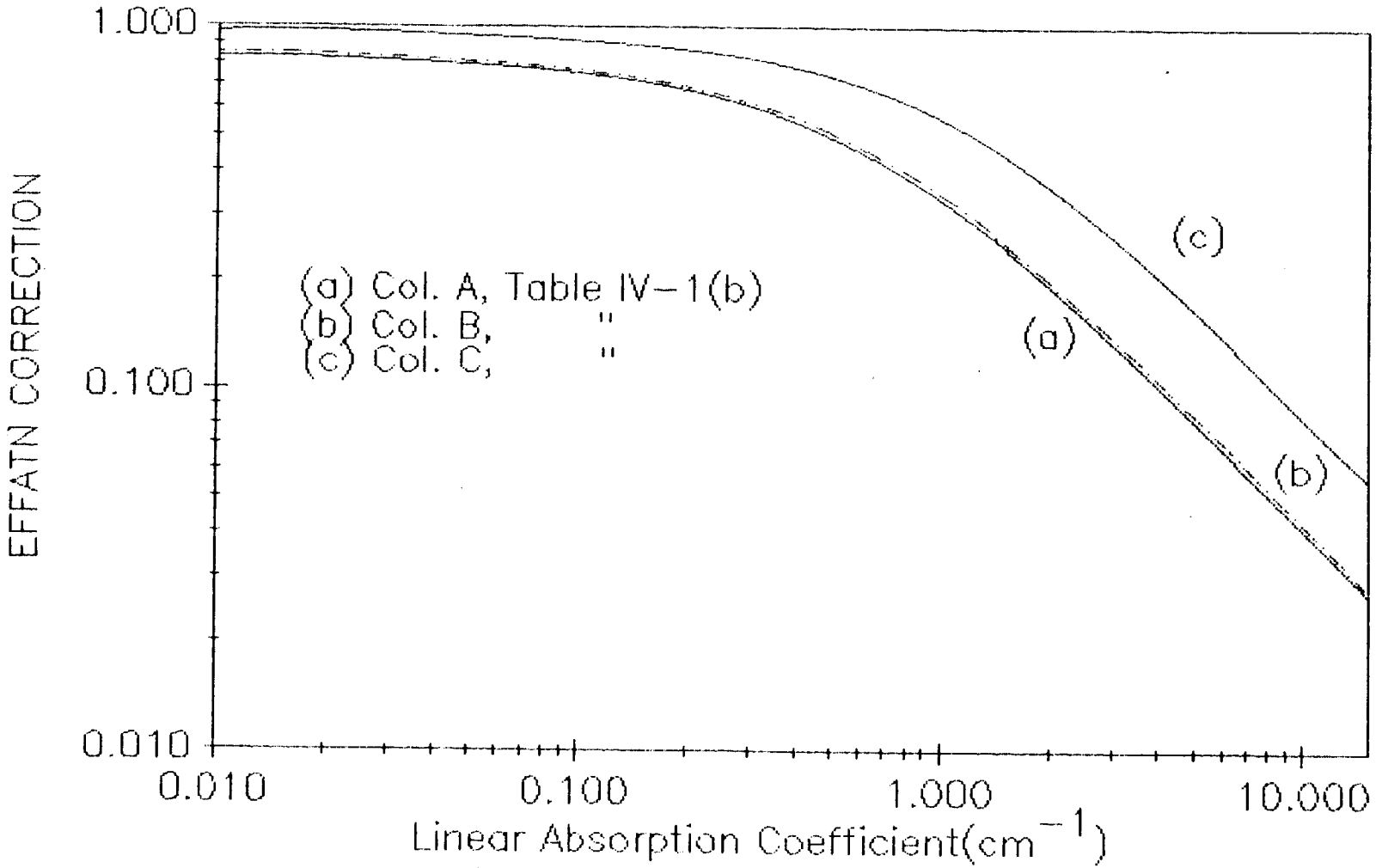

Figure IV--1(d) EFFATN Correction for Cylinder Samples

Figure IV--2 Efficiency Curve for S/L Detector

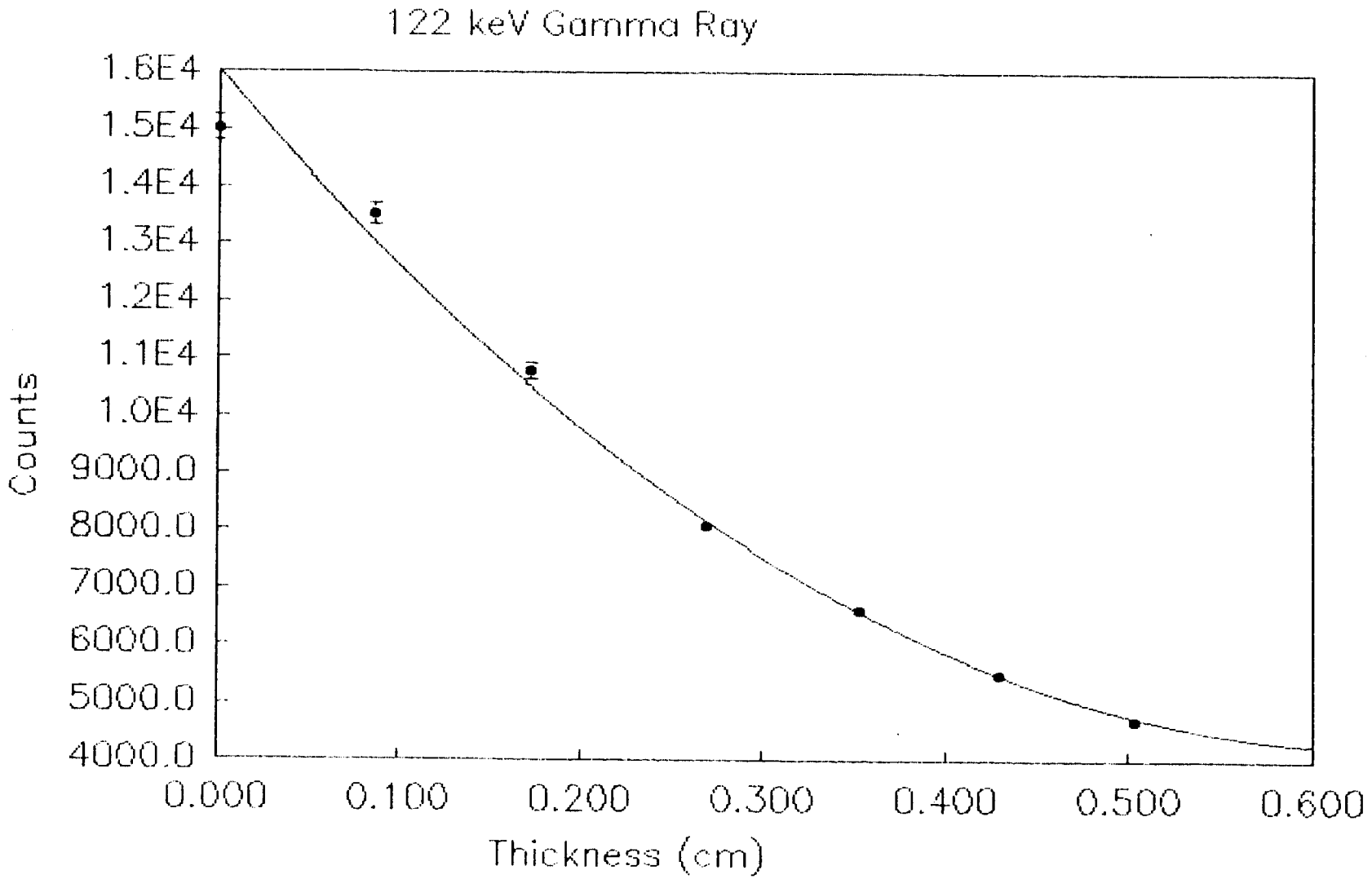

Figure IV–3(a) Yield of 122 keV Gamma Ray vs. EFFATN Prediction

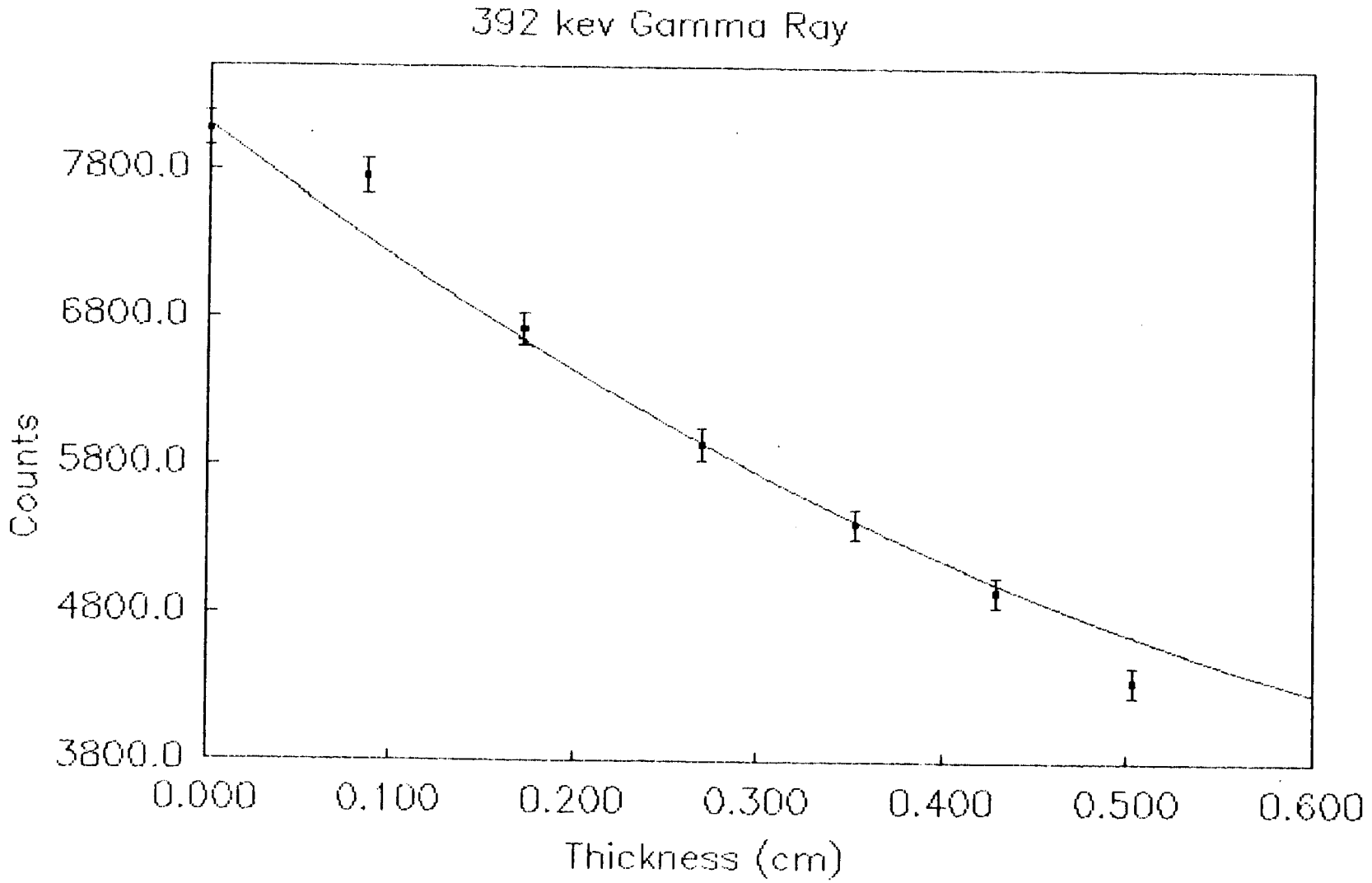

Figure IV–3(b) Yield of 392 keV Gamma Ray vs. EFFATN Prediction

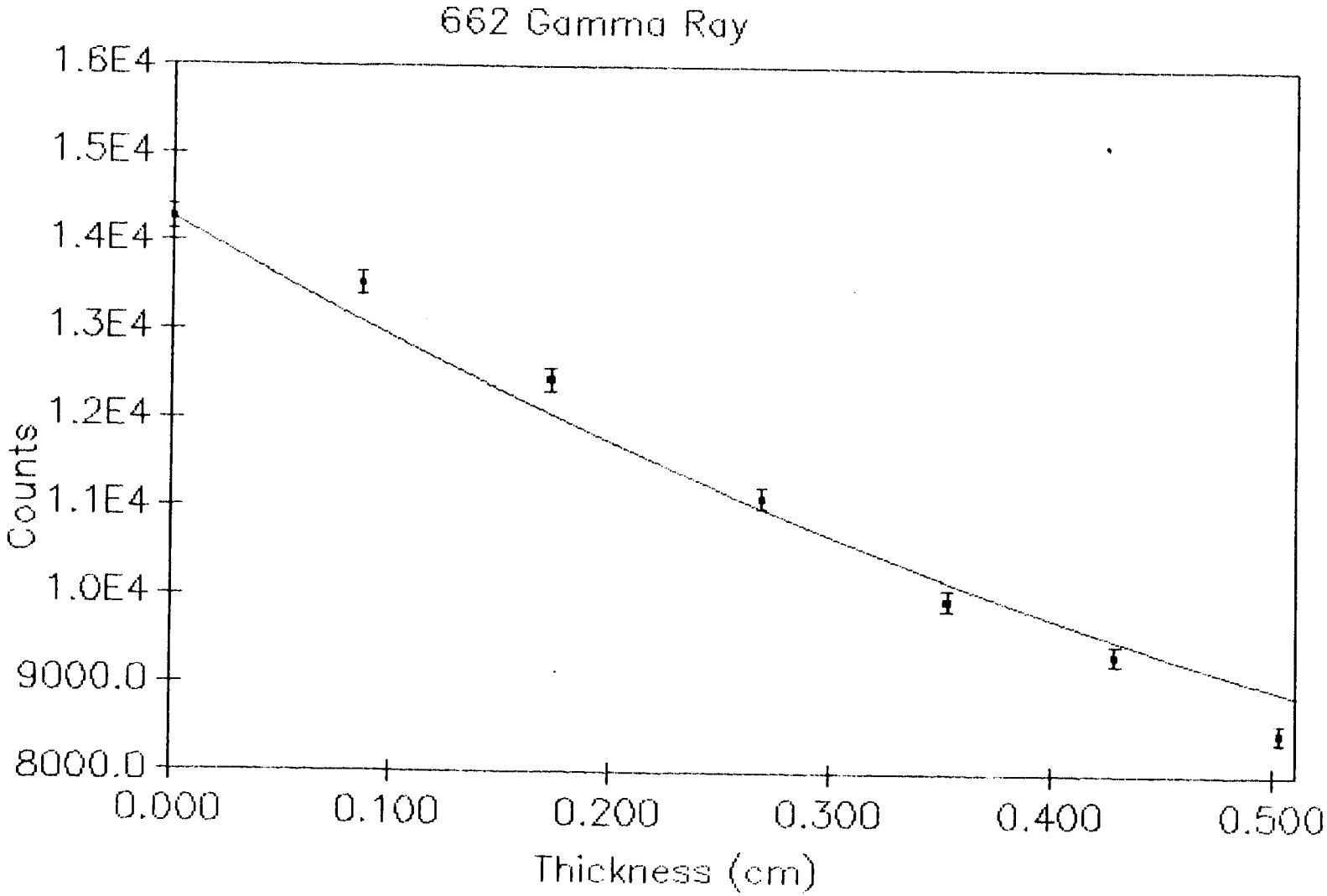

Figure IV-3(c) Yield of 662 keV Gamma Ray vs. EFFATN Prediction

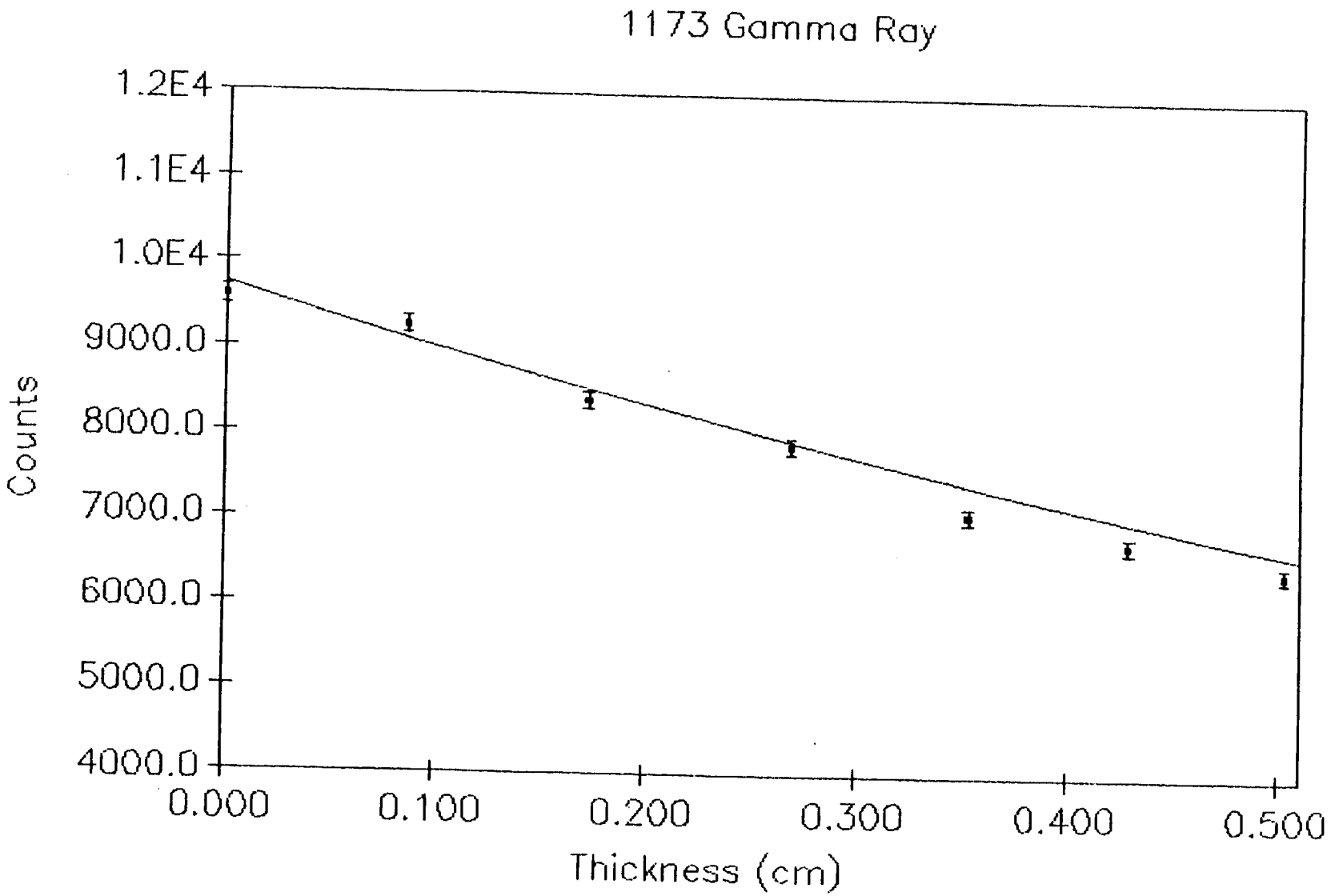

Figure IV–3(d) Yield of 1173 keV Gamma Ray vs. EFFATN Prediction

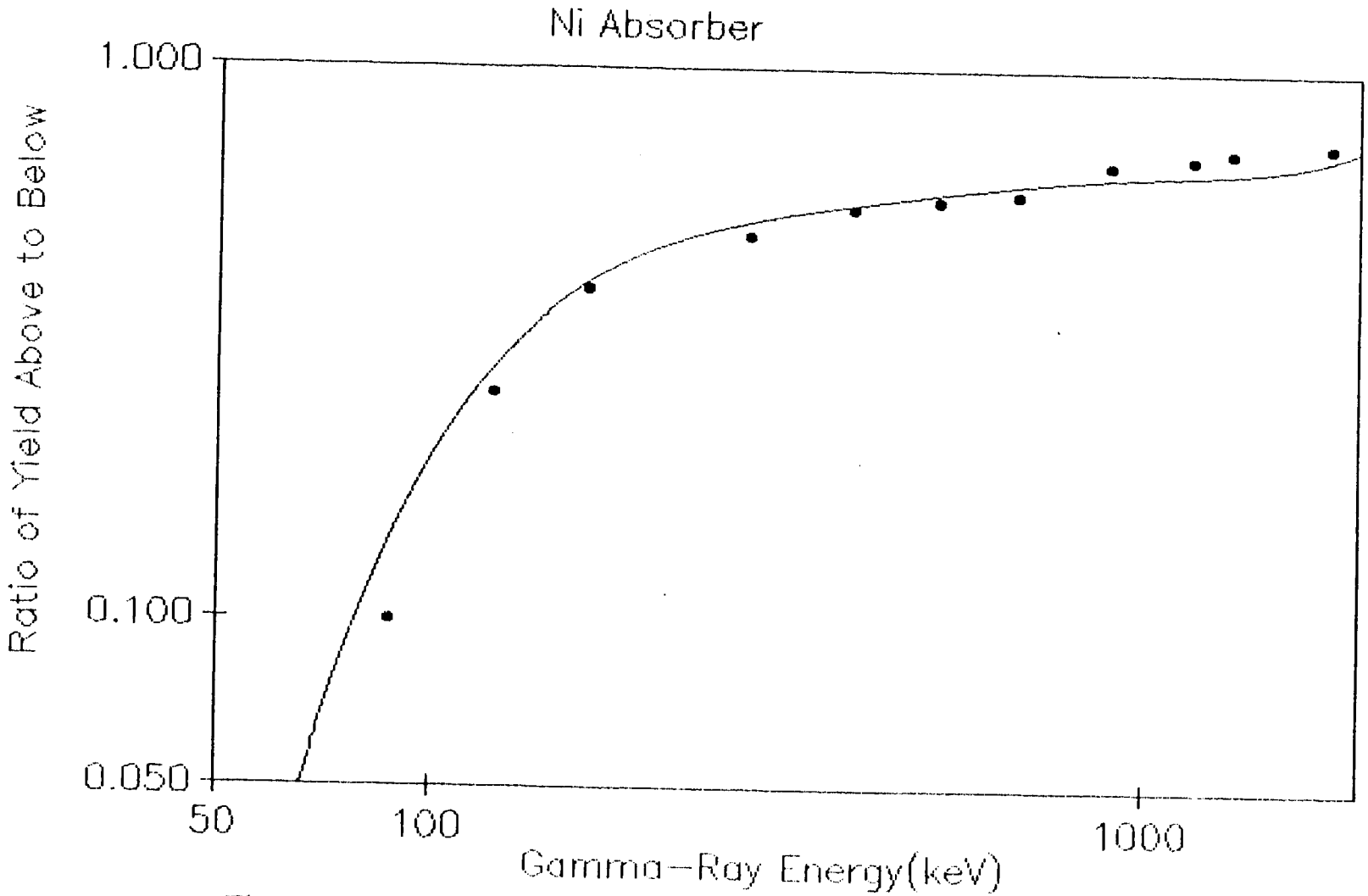

Figure IV-4 JSC Absorption vs. EFFATN Correction(line)

V. Present Status of Sample Counting

Dr. Gerald Fishman at the Space Science Laboratory, Marshall Space Flight Center, has obtained samples from the LDEF other than the intentional samples originally placed aboard it. The new samples obtained from other experiments and the structure itself, include, but are not limited to, experimental plates and trays, stainless steel trunnions, screws, tray clamps, ballast and bolts. In total, more than 400 samples have been selected for possible study. Included in this material are the elements titanium, iron, nickel, copper, chromium, germanium, lead, and aluminum.

Dr. Alan Harmon, a colleague of Dr. Gerald Fishman at the Marshall Space Flight Center, has been assigned the responsibility for distributing the sample materials retrieved from LDEF for low-background gamma-ray counting at the following facilities:

Batelle Northwest
Johnson Space Center
Marshall Space Flight Center
Lawrence Livermore National Laboratory
Lawrence Berkeley Laboratory
Los Alamos National Laboratory
Savannah River-Westinghouse
Tennessee Valley Authority.

All of these facilities have well-shielded large-volume germanium photon detectors used for low-background counting. The arrangement of these facilities vary from those buried underground in specially designed rooms or under dams to well-shielded ground-level facilities. The laboratories will count the assigned samples and, given reasonable geometries, are to correct for efficiency, solid angle, and self-attenuation effects. Results are to be reported in terms of pico-Curies of activity(.037 decays per second) per kilogram of sample material. Also, the results are to be corrected for decay back to January 20, 1990 which has been chosen as the reference date for LDEF retrieval. Samples are to be rotated between counting facilities so that differences in results can be identified and the analyses studied for systematic errors.

As of December 31, 1990 the counting of all of the intentional samples and of those samples such as trunnion sections for which absolute activities can be readily calculated was still on-going. With typical total counting times of six to nine days for each sample, with

about three gamma-ray spectra for each sample to be analyzed for yields and corrected for efficiency and self-absorption, and with an average of about 200 samples to be counted at each facility, it is not surprising that results from the laboratories were incomplete after only nine months from the distribution of samples. Although some laboratories have analyzes many of the samples they had counted, none have completed the process. Most of the laboratories have not had sufficient time to complete this process. Tabulations of these results has begun but is currently incomplete. The search for systematic differences in the data awaits the completed tabulation.